

# Rip It, Stitch It, Click It: A Chemist's Guide to VLP Manipulation

Fabian C. Herbert,<sup>a,†</sup> Yalini H. Wijesundara,<sup>a,†</sup> Sneha Kumari,<sup>a</sup> Thomas Howlett,<sup>a</sup> Shailendra Koirala,<sup>a</sup> Orikeda Trashi,<sup>a</sup> Ikeda Trashi,<sup>a</sup> Noora M. Al-Kharji,<sup>a</sup> and Jeremiah J. Gassensmith.<sup>a,b,\*</sup>

- a) Department of Chemistry and Biochemistry, The University of Texas at Dallas, 800 West Campbell Rd. Richardson, TX 75080, United States.  
E-mail: [gassensmith@utdallas.edu](mailto:gassensmith@utdallas.edu)
- b) Department of Biomedical Engineering, The University of Texas at Dallas, 800 West Campbell Rd. Richardson, TX 75080, United States.

## Abstract

Viruses are some of nature's most ubiquitous self-assembled molecular containers. Evolutionary pressures have created some incredibly robust, thermally and enzymatically resistant containers to transport delicate genetic information safely. Virus-like particles (VLPs) are human-engineered non-infectious systems that inherit the parent virus' ability to self-assemble under controlled conditions while being non-infectious. VLPs and plant-based viral nanoparticles are becoming increasingly popular in medicine as their self-assembly properties are exploitable for applications ranging from diagnostic tools to targeted drug delivery. Understanding the basic structure and principles underlying the assembly of higher-order structures has allowed researchers to disassemble (rip it), functionalize (click it), and reassemble (stitch it) these systems on demand. This review focuses on the current toolbox of strategies developed to manipulate these systems by ripping, stitching, and clicking to create new technologies in the biomedical space.

**Key words:** Virus, virus-like particles, self-assembly, disassembly, non-infectious, drug delivery.

## Introduction

Supramolecular self-assembly is a common approach to formulating nanomaterials, and using (Yadav et al., 2020) diverse molecular building blocks such as lipids, (Felice et al., 2014; Lee, 2008; Xing and Zhao, 2016) metals, (Katayama et al., 2019) proteins, (McManus et al., 2016; Sun et al., 2020; Wang et al., 2020) and polymers. (George et al., 2019; Nitta and Numata, 2013; Sofi et al., 2019; Wang et al., 2017a) It is possible to synthesize varied and functional nanostructures with these building blocks that bear unique physicochemical properties. The higher-order structure and emergent function obtained from these nano-assemblies have opened the door for addressing complicated problems in drug delivery, (Vilar et al., 2012; Wang et al., 2016; Wang et al., 2018) catalysis, (Brea et al., 2010) and targeting of biomaterials for therapeutic applications. (Cheng et al., 2020) Generally, self-assembly is a spontaneous process where thermodynamically favorable interactions occur amongst unorganized subunits to ultimately give rise to ordered structures. While synthetic systems—particularly in organic solvents—are enthalpically driven by forces like hydrogen bonding or  $\pi$ -stacking, biological systems typically

are driven entropically, as self-assembly in aqueous systems often results in the release of ordered water around hydrophobic residues.(Jiou et al., 2014; Mendes et al., 2013; Schmit et al., 2010) Nature has exploited these driving forces for billions of years to create living beings—beings that have begun to create new materials using inspiration from the elegance of biological self-assembly.(Pochan and Scherman, 2021) Development of the cell membrane through the interaction of phospholipid bilayers,(Ng et al., 2004) protein folding,(Levin et al., 2020) and DNA arrangement(Krissanaprasit et al., 2021) are just a few examples of how self-assembly governs the emergence and maintenance of life within biological systems.(Wang et al., 2017b) Further, self-assembly is pivotal in acquiring structured materials such as phase-separated polymers, liquid crystals, and crystalline polymers.(Yadav et al., 2020)

Self-assembled proteinaceous structures have been extensively investigated for the development of bio-functional materials. The rational design of protein-protein interactions is very complex and predicting how proteins assemble is still a developing field. As a result, proteinaceous nanomaterials are engineered mainly based on existing self-assembled systems like viruses,(Bai et al., 2008) chaperones,(Geitner and Schmid, 2012) amyloids,(Díaz-Caballero et al., 2021) elastin,(Le et al., 2013) resilin,(Renner et al., 2012) and silk-like proteins.(Kluge et al., 2008) By using naturally occurring self-assembling proteins as a starting point, it has become possible for proteinaceous materials to be used as scaffolds to construct various supramolecular interfaces.(Solomonov and Shimanovich, 2020) For instance, protein-based nanomaterials display structural features with great potential for the fabrication of drug delivery systems,(Zdanowicz and Chroboczek, 2016) imaging agents,(Schwarz and Douglas, 2015) targeting agents,(Suffian and Al-Jamal, 2022) and vaccines.(Roldão et al., 2010)

Viruses are some of nature's most resilient self-assembled nanostructures that have been exploited in their non-infectious forms for various applications. Recent work on controlling their assembly, disassembly, and chemical functionalization have created a new field—Chemical Virology—that seeks to understand the complexities of self-assembly with proteins and exploit these structures for application in medicine and materials. In this review, we focus specifically on virus-like particles (**VLPs**) and plant viruses, a family of proteinaceous materials whose cargo-loading ability and biocompatibility have piqued the interest of researchers involved in the development of therapeutics and prophylactics.

## **Virus-like Particles**

VLPs are proteinaceous materials derived from viruses that can self-assemble but lack the genetic material needed for their replication within the host cell.(Zhao et al., 2019) Genetic engineering and self-assembly are two of the most common methods employed to fabricate these virus-like particles from their parental virions. The viral genetic code is responsible for determining the protein composition of the viral capsid, and researchers have been using genetic engineering and bioinformatics to modify the protein capsids to create biodegradable and non-toxic nanomaterials.(Jeevanandam et al., 2019) Today, CRISPR/Cas9-based gene editing is one of the most widely used genetic engineering techniques to produce VLPs from viruses.(Jeevanandam et al., 2019; Teng et al., 2021) When genetic engineering cannot introduce the desired function, chemical bioconjugation is used to modify or target both natural and synthetic amino acid residues on the protein capsid of the VLPs.(Biabanikhankahdani et al., 2018) In this

way, VLPs have emerged as a semi-synthetic biological material that has shown promise in areas as diverse as enzymatic reactors to imaging agents.(Herbert et al., 2020; Pokorski et al., 2011; Waghvani et al., 2020) VLP expression and *in vitro* self-assembly can be achieved through various host systems such as bacterial, plant, yeast, mammalian, and insect cells.(Liu et al., 2016) The capsid self-assembly happens when VLP subunits and other viral components interact to minimize the free energy required to construct high-order structures.(Garmann et al., 2019) Capsid formation is a multistep process that begins with a nucleation phase, where a capsid oligomer is formed.(Le and Müller, 2021) This is followed by the growth phase, where VLP subunits interact.(Hagan, 2014; Perlmutter and Hagan, 2015) Finally, the capsid is created via the interaction of smaller building blocks resulting in a highly ordered structure.(Hagan and Elrad, 2010) Though favorable, this assembly process can be complicated and vary from VLP to VLP.(Chi et al., 2003)

VLPs have recently gained popularity in medicine as their self-assembly properties are exploitable for various applications ranging from diagnostic tools in non-invasive imaging(Herbert et al., 2020) to drug delivery.(Lee et al., 2018) They are also popular vaccine candidates, as many of these proteinaceous materials are intrinsically immunogenic and can elicit potent humoral and cell-mediated immune responses.(Luzuriaga et al., 2021; Shahrivarkevishahi et al., 2022; Welch et al., 2018) Compared to other commonly used nanoparticles such as liposomes, lipid-based nanoparticles, and dendrimers, many VLPs allow orthogonal surface modifications to install more than one new chemical moiety.(Benjamin et al., 2020b; Shahrivarkevishahi et al., 2021) For instance, drug delivery components can be installed via a single set of reactions, and stealth PEG coatings that promote solubility can orthogonally be attached to the same VLP via a second reaction. VLPs are also structurally rigid enough that their tertiary and quaternary structures can actively template the formation of new nanomaterials, such as gold nanoparticles and Metal-Organic Frameworks (**MOFs**).(Benjamin et al., 2018) Additionally, VLPs can be disassembled/reassembled *in vitro*, allowing foreign materials to be encapsulated within their capsid.(de Ruiter et al., 2019) In return, the encapsulated material can be protected from harsh conditions (e.g., nuclease degradation), and its cellular delivery is controlled through elegant surface modification of the capsid.(Rhee et al., 2011)

### **Structural Diversity of VLPs**

The self-assembly of VLPs is a diverse, synergetic, and multiprotein process. Though highly complex, much has been gleaned from biophysical studies, such as isothermal titration calorimetry (**ITC**),(Jeembaeva et al., 2010; Nebel et al., 1995) to monitor heat dissipation upon association of different VLP subunits. Studies performed by Maassen *et al.* quantitatively and qualitatively investigated the impact of associations between coat proteins (**CPs**) and cargo (e.g., single-stranded DNA) on the stability of VLPs. (Maassen et al., 2019) Their work shows that the self-assembly of VLPs results from the electrostatic interactions between CPs and different cargo and protein-protein associations, primarily dependent on hydrophobic interactions. When hydrophobic surfaces interact, they release large amounts of highly structured water. Consequently, even though the capsid becomes more ordered, the overall system has higher entropy. Interestingly, these weak hydrophobic interactions are non-directional—unlike non-covalent supramolecular bonds like hydrogen bonding—yet these forces drive the formation of VLPs with different geometries, including rod-like, icosahedral, or spherical.(Zeltins, 2013) This

review will mainly focus on seven very simple viruses—illustrated in Figure 1. These systems have been utilized broadly and are relatively simple—they lack a lipid membrane (*i.e.*, non-enveloped), and few proteins are involved in their formation. We will cover their laboratory purification and characterization techniques and post-synthetic modifications (e.g., self-assembly, disassembly, and bioconjugation).

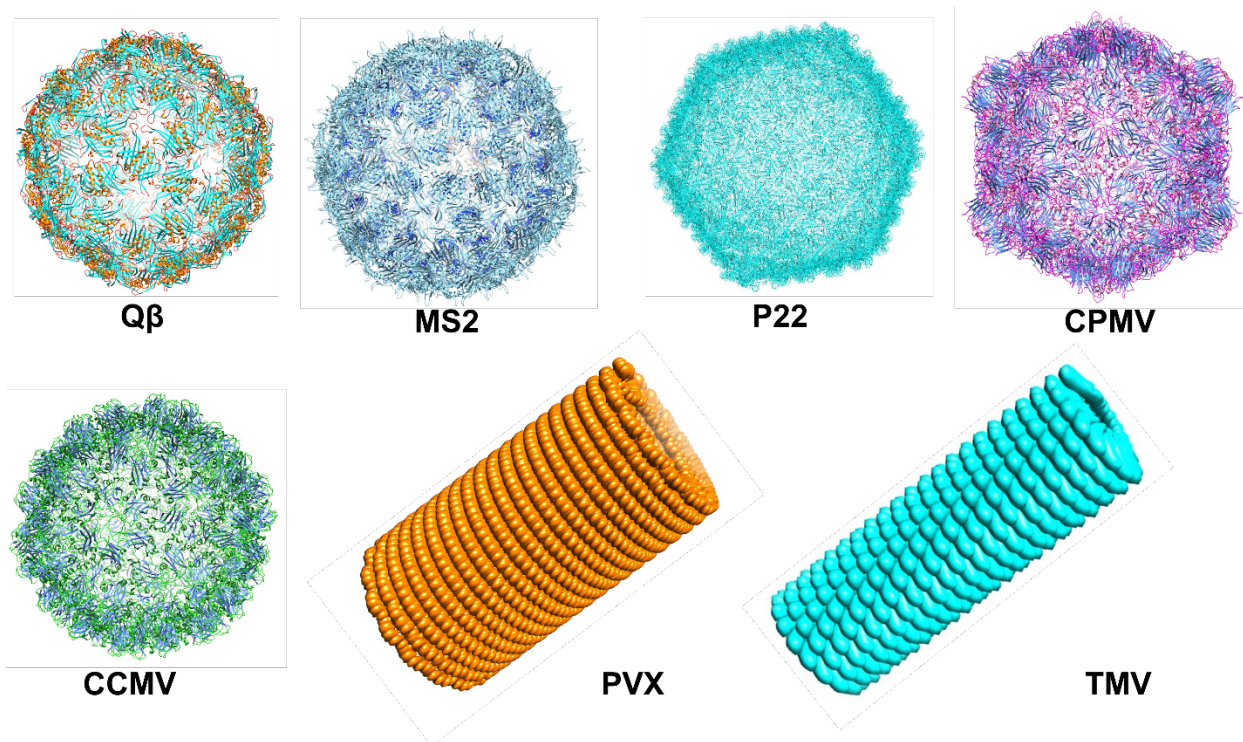


**Figure 1.** Structural diversity of commonly reported icosahedral and rod-shaped virus-like particles and viruses.

### Commonly reported Virus-like Particles

The architectural diversity of VLPs provides researchers with different options for designing hybrid materials.(Chung et al., 2020) Here, we summarize commonly used VLPs that have been extensively exploited to develop bio-functional nanomaterials.

**Bacteriophage Q $\beta$  (Q $\beta$ )** is a porous icosahedral VLP with a 28-30 nm diameter.(Benjamin et al., 2018) Q $\beta$  is a member of the *Leviviridae* family,(Herbert et al., 2020) a group of phages that display a 4.2 kilobase single-stranded RNA (**ssRNA**) genome,(Cui et al., 2017) a capsid built from 180 copies of a 14 kDa CP,

(Sungsuwan et al., 2017) .(Lee et al., 2018) Bacteriophages belonging to the *Leviviridae* family are characterized by a capsid comprising a major CP and one or two species of minor structural proteins responsible for genome packing and recognition. Further, these supporting structural proteins are essential for absorbing the virion to cell receptors and transporting the RNA genome into the gram-negative bacterial cells; however, they are not required for the assembly or structural integrity of the viral capsid. As a result, recombinant expression of a cloned version of the major CP results in the production of Q $\beta$  VLPs.(Kozlovska et al., 1993) The resulting VLP

only has 180 copies of a single CP, as opposed to the native (or wild-type) virus, which has additional proteins used to infect its host, *E. coli*. The positively charged inner surface of this CP plays a pivotal role in its self-assembly into the Q $\beta$  capsid, as it binds bacterial RNA, driving the formation of intact capsids during recombinant expression in *E. coli*.(Herbert et al., 2020) Q $\beta$  has been extensively investigated as a drug delivery vehicle,(Chen et al., 2017) cancer therapeutic,(Shahrivarkevishahi et al., 2021) and has performed well in clinical trials when used with immunoadjuvants.(Lemke-Miltner et al., 2020) The outstanding overall pre-clinical performance of Q $\beta$  can be attributed to its biodegradability, biocompatibility, and presence of surface functional handles.(Benjamin et al., 2020b) Q $\beta$  displays three surface-exposed lysine residues and two surface-exposed cysteine residues on each CP,(Au - Chen et al., 2018; Chen et al., 2016; Shahrivarkevishahi et al., 2021) which have facilitated multiple orthogonal surface modifications.

**P22** is a bacteriophage whose native host is *Salmonella typhimurium*. It was found that its assembly and maturation depend on two major components – a 47 kDa CP which is responsible for the formation of the capsid shell, and a 33.6 kDa scaffolding protein (**SP**) which acts as a template and direct CPs for proper assembly into a VLP when recombinantly expressed in *E. coli*.(Kutter, 2001) (Patterson, 2018) The P22 capsid was the first bacteriophage shown to perform generalized transduction – a process where the virus transfers its genetic material into a bacteria. This finding opened various research avenues for developing phage-mediated transfer of genetic material.(Casjens and Grose, 2016) In 1973, Lobban and Kaiser demonstrated the first use of bacteriophages as DNA cloning vectors using P22.(Petes et al., 1978) The structure of the P22 VLP is first built by the assembly of 250 SP units to form a procapsid, which is subsequently disassembled for the DNA to enter. These SPs are the precursors for the self-assembly of the 420 CPs, forming the VLP. It is worth noting that only the last few C-terminal residues of the SP are required for facilitating capsid formation.(Moore and Prevelige, 2002) As a result, many groups have taken advantage of this to fuse enzymes or proteins to P22 capsids.(Seul et al., 2014) These stylish genetic alterations have allowed P22 to be used in cargo loading(Sharma et al., 2017) and imaging applications.(Lucon et al., 2012a)

**Bacteriophage MS2** is another icosahedral RNA phage member of the *Leviviridae* family.(Salas and de Vega, 2008) MS2 is known to infect *E. coli*,(Salas and de Vega, 2008) and hence found its original use as an indicator virus at waste management plants for determining *E. coli* contamination levels.(Farkas et al., 2020) Self-assembly of MS2 affords icosahedral particles of 29 nm in diameter.(Biela et al., 2022) The genome of MS2 is composed of a positive-sense ssRNA with 3,569 nucleotides which encode four proteins: the major CP, the replicase, the lysis, and the maturation protein. (Fu and Li, 2016) Further, recombinant expression of cloned CPs will promote the self-assembly of MS2 VLP.(Mastico et al., 1993) The resulting capsid is known for its outstanding stability, making it an excellent model for studying factors affecting capsid integrity (e.g., pH, temperature, and ionic strength).(Caldeira and Peabody, 2011; Furiga et al., 2011; Hashemi et al., 2021) This structural feature has been exploited for *in vitro* capsid disassembly/assembly, which has found use in drug delivery.(Ashley et al., 2011) MS2 is also suitable for genetic modification through the insertion of peptides into the N terminus of the CP.(Tumban et al., 2012) This strategy, in particular, has been exploited for multiple epitope presentations in the field of vaccine research.(Peabody et al., 2008)

Similar to VLPs, plant viral nanoparticles (**VNPs**) have emerged as self-assembling nanostructures.(Martí et al., 2022) Unlike VLPs, VNPs are active and infectious viruses; most work done with VNPs has focused on plant viruses, which are incapable of causing disease in mammalian cells or tissue. VNPs are just as structurally diverse as engineered and non-infectious VLPs; some display structural similarities (e.g., size and shape) to icosahedral bacteriophages, whereas others are helical-shaped.(Chung et al., 2020) VNPs are widespread in crops across the globe, including fruits and vegetables, and can seriously threaten agricultural production.(Rubio et al., 2020) However, these are only infectious to plants, making their application in mammalian-based medicine possible.(Steinmetz, 2010) It is worth pointing out that literature often uses the two terms interchangeably, though the distinction that VNPs are infectious is essential.

**Cowpea mosaic virus (CPMV)** is a picorna-like virus of the order *Picornavirales*, family *Secoviridae*, and genus *Comoviridae* that naturally infects the black-eyed pea plant *Vigna unguiculata*.(Hesketh et al., 2017) CPMV is a 30 nm isometric, icosahedral lattice capsid with a pseudo T = 3 quasi symmetry, and a net negative surface charge.(Patel et al., 2020)The capsid shape provides a large surface area-to-volume ratio, which is advantageous for enhanced multifunctional group display and cargo-loading capacity. CPMV has a bipartite, positive-sense RNA genome comprised of RNA-1 (5.89 kbp) and RNA-2 (3.48 kbp) encapsulated separately.(Rae et al., 2008) The icosahedral capsid allows for enhanced multifunctional group display and the ability to carry specific cargoes.(Sainsbury et al., 2010) The native tropism of CPMV for cell surface displayed vimentin—a type III filament upregulated in cancer progression—and the enhanced permeability and retention effect allows them to extravasate from the tumor neovasculature and efficiently penetrate them preferentially.(Beatty and Lewis, 2019)

**Cowpea Chlorotic Mottle Virus (CCMV)** is an icosahedral, non-enveloped member of the Bromoviral family of plant viruses that infects cowpea plants.(Wilts et al., 2015) The CCMV capsid is 28 nm in diameter, icosahedral in shape, and self-assembles from the interaction of 180 CPs.(Konecny et al., 2006) Capsid particles are stabilized through RNA-protein interactions.(Konecny et al., 2006) These interactions are driven through the anionic RNA and the inner positive charge of capsid proteins.(Konecny et al., 2006) CCMV is notorious for its structural dynamism – a structural feature that makes it a very attractive VNP for post-expression modifications.(Liepold et al., 2005) For example, the capsid can undergo pH-dependent swelling, allowing for entrapment of foreign material within CCMV without the need for *in vitro* disassembly/reassembly.(Wilts et al., 2015) Finally, the capsid displays several functional handles used for conjugation approaches. (Vervoort et al., 2021)

**Tobacco Mosaic Virus (TMV)** was the first virus to be discovered and was instrumental in shaping virology as a field.(Van Regenmortel, 2008) It has a helical rod shape of 300 nm in length and 18 nm in diameter.(Hema et al., 2019) Despite its stability, the virus has been known to mutate in the laboratory environment, though mutations are easily detected via electrospray mass spectrometry (ESI-MS).(Lumata et al., 2021) The three-dimensional structure of TMV has been extensively characterized using X-ray crystallography and cryo-electron microscopy (**Cryo-EM**).(Muller, 1999) The outer surface of TMV is made of 2,130 CPs, each having 158 amino acids.(Hema et al., 2019) The inner part has a diameter of 4 nm, and a viral ssRNA made of 6,400 nucleotides is located at the center of the helix, giving TMV its ability to replicate in host

cells.(Lomonosoff and Wege, 2018) Further, the biodegradability and biocompatibility of TMV plus its structural features have been widely exploited for MRI imaging applications and other modalities.(Bruckman et al., 2013; Niehl et al., 2016; Wang et al., 2019)

**Potato Virus X (PVX)** belongs to the family *Alphaflexiviridae* and is a member of the genus *Potexvirus*. It is a flexuous filamentous rod having a length of 515 nm, a diameter of 13 nm, and monopartite positive-sense ssRNA. It has 1,270 identical CPs with a molecular weight of 25 kDa arranged around the 6.4 kbp ssRNA.(Lico et al., 2015) The C-terminus of each CP subunit is located within the particle. In contrast, the N-terminus is exposed and can be easily modified at the genetic level to display amino acids or small peptides. It displays a helical array (3.6 nm pitch) with the viral RNA packed between the helix turns. There are 8.9 CP subunits (each consisting of 236 amino acid residues) per turn of the primary helix. The relative molecular weight of the virion( $M_r$ ) is about 3,500 kDa. Other important physical properties of PVX include a sedimentation coefficient ( $S_{20w}$ ) of 115–130S, a buoyant density in CsCl of 1.31 g/cm<sup>3</sup>. The ssRNA represents about 6% of the weight of the virion.(Grinzato et al., 2020)

### Commonly used expression systems to produce icosahedral VLPs and rod-like viruses.

Expression systems of eukaryotic and prokaryotic origin are commonly employed to produce VLPs.(Arevalo et al., 2016) The two standard eukaryotic systems used to produce VLPs are plant and mammalian cell cultures. The most used prokaryotic system is bacteria, specifically *E. coli*. Selection of the appropriate expression system is imperative for the production of VLPs. In this section we discuss some of the commonly used expression systems and have gone in detail with the most popular approach for each VLP/VNP. (remove the reference from the list)

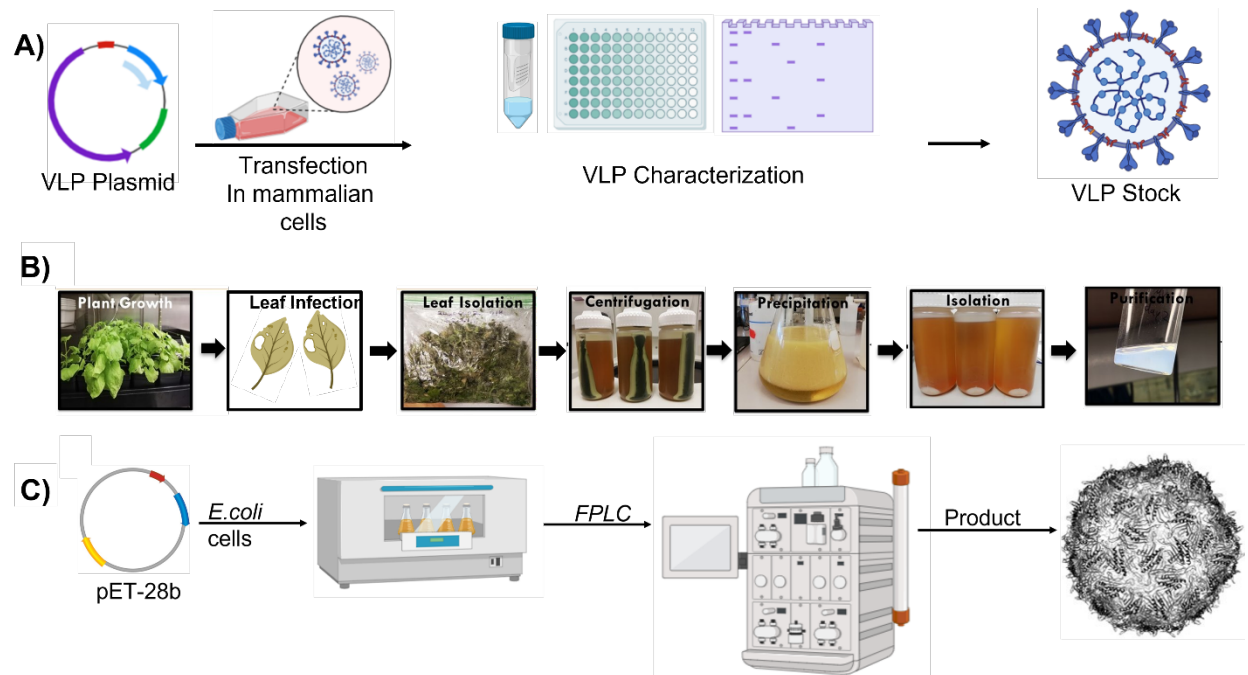


**Figure 2. Common platforms for the expression of VLPs and viruses.** A) Mammalian VLP and viral expression. B) Plant-based expression of viruses (e.g., TMV). C) Bacterial culture expression using BL21 (DE3) cells.

### **Mammalian cell culture**

Though this review does not cover VLPs or VNPs typically produced in mammalian cell culture, it is an essential method for making many types of VLPs/VNPs used in vaccine and gene transfection. These platforms are attractive for producing various VLPs, because they can accommodate post-translational modifications needed within the cell (e.g., methylation, acetylation, hydroxylation, and phosphorylation) for proper capsid formation. Additionally, this method of expression is most suitable for creating complex enveloped VLPs comprised of multiple structural proteins.(Fuenmayor et al., 2017) However, this expression system is notorious for lower VLP yields than other platforms such as *E. coli*.(Fuenmayor et al., 2017) Some popular cell lines used for VLP expression include human embryonic kidney 293 (HEK293), Chinese hamster ovary (CHO), and baby hamster kidney-21 (BHK-21).(Nooraei et al., 2021) These cell lines have been widely employed for VLPs, such as influenza, HIV, and rabies.(Cervera et al., 2013; Fontana et al., 2015; Thompson et al., 2013)

### **Plant culture**

Plant-based VLP production systems offer advantages over other commonly used approaches. For example, plants offer high protein expression levels, cheap maintenance, and ease of purification.(Nooraei et al., 2021) The most popular plants used for expressions of VLPs and VNPs are *Solanum lycopersicum*,(Saldaña et al., 2006) *Solanum tuberosum*,(Warzecha et al., 2003) *Arabidopsis thaliana*, and *Nicotiana tabacum*.(Greco et al., 2007) In particular, *Nicotiana benthamiana*—a small plant from Australia—is characterized by several traits, including the ability to host expression of heterologous gene sequences and a fast growth rate.(Goulet et al., 2019) The typical laboratory strain has retained a loss-of-function mutation in Rdr1 (RNA-dependent RNA polymerase 1), making it a popular platform for expressing numerous VNPs.

### **Bacterial culture**

Bacterial expression systems are commonly employed to produce recombinant proteins and VLPs. These expression systems are popular for their low cost and high protein expression yields.(Nooraei et al., 2021) However, this method is unsuitable for VLPs that could require post-translational modifications.(Fuenmayor et al., 2017) Other factors that challenge bacterial expression systems are protein solubility and incomplete disulfide bond formation.(Naskalska and Pyrc, 2015) Most commonly used bacterial strains for VLP expression include DH5 $\alpha$ , BL21 (DE3), and clear *E. coli*.(Au - Chen et al., 2018; Shahrivarkevishahi et al., 2021). Further, these strains tend to be transformed via heat shock or electroporation(Rahimzadeh et al., 2016) and can be grown using different media such as Lysogeny broth (LB) or Super Optimal broth (SOB).

**Purification, functionalization, and characterization techniques used for icosahedral VLPs and rod-like viruses.**

This section focuses on the expression and characterization of VLPs and their chemical functionalization – most of these processes are relatively straightforward. VLPs are generally resistant to proteases and are thermally robust. Hence, they can be prepared and purified at room temperature in most cases with minimal or no chromatography. Chemical modification of the VLPs is likewise straightforward and often very high yielding; however, functionalization with hydrophobic molecules can occasionally cause precipitation. Strategies to overcome this include orthogonally attaching solubilizing PEG linkers or reducing the number of equivalents used to functionalize the surface. To keep the discussion concise, we have included tables of methods used to functionalize the previously discussed VLPs with various moieties.

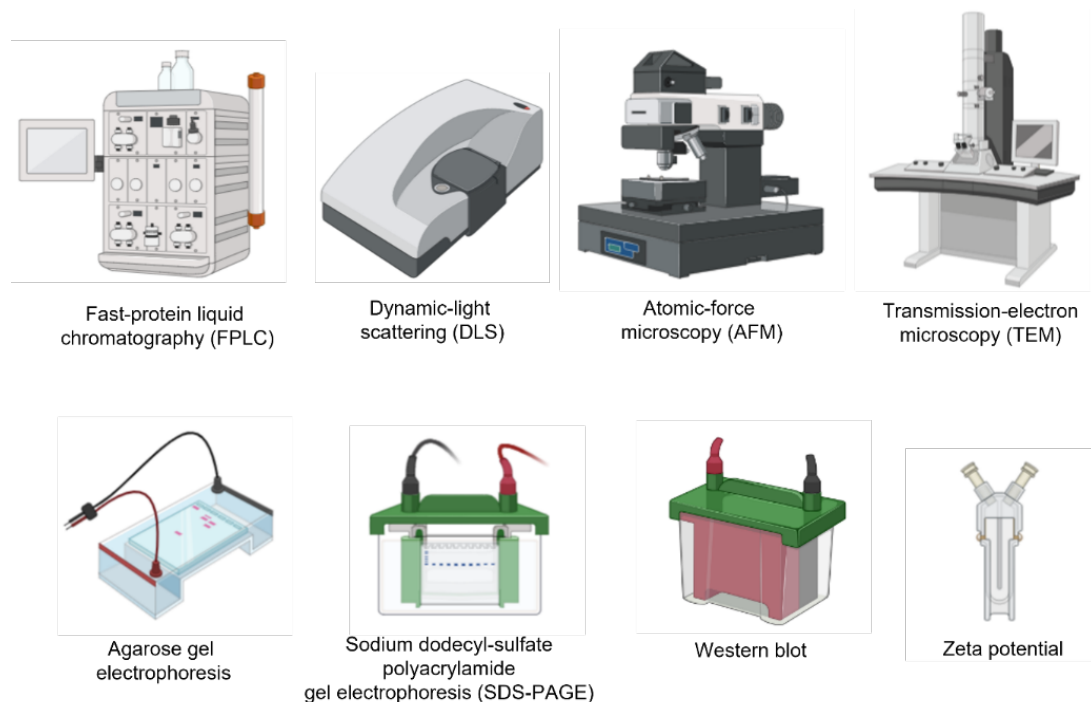


**Figure 3.** Post-expression characterization techniques for VLPs and viruses.

Depending on the type of VLP or VNP used, different purification and characterization techniques are employed following the expression of these materials. While some of these techniques overlap, others differ significantly. We hope the following section of our review serves as a template to instruct new and experienced users on what techniques to use for optimizing their VLP and/or VNP production.

### Post-synthetic modifications of VLPs and viruses

A notable characteristic of viruses and VLPs is their ability to be post-synthetically modified. For example, these proteinaceous materials display a wide range of surface-exposed amino acids which can be used for bioconjugation reactions. (Benjamin et al., 2020a) Bioconjugation strategies have recently gained much attention, as they can be used for tailoring VLPs and VNPs to perform specific functions such as imaging, cellular trafficking, and targeted drug delivery. (Shahrivarkevishahi et al., 2022) Though convenient, these reactions are not simple to execute in cases where the availability of exposed amino acids is limited, resulting in reduced

efficiency of bioconjugation.(Hermanson, 2013) Figure 4 highlights some approaches to decorate the surface-exposed amino acids found in VLPs and viruses.(Benjamin et al., 2020a)

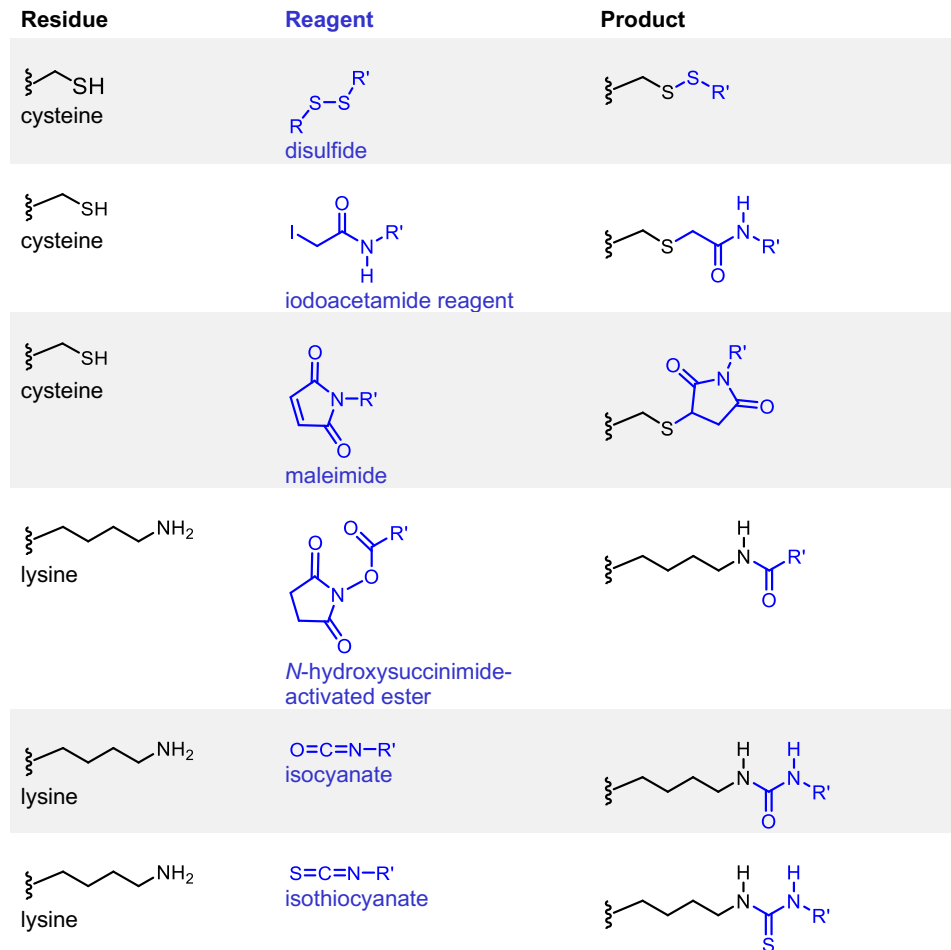


**Figure 4.** Common amino acids targeted for bioconjugation techniques in VLPs and VLPs.

## Q $\beta$

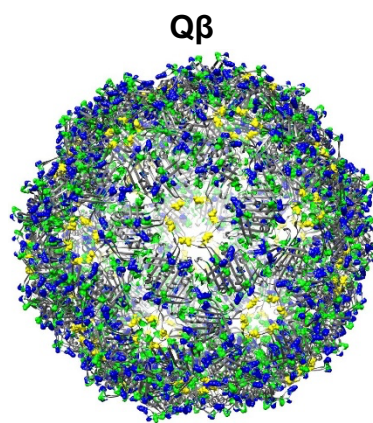
Recombinant expression of Q $\beta$  (e.g., pET28 wtQ $\beta$ ) begins with the transformation of the plasmid into DH5 $\alpha$  – bacterial cells commonly employed for cloning and plasmid maintenance. When ready for expression, the Q $\beta$  is transformed into BL21 (DE3) or clear *E. coli*.(Brown et al., 2009) Q $\beta$  can be expressed using either LB or SOB and appropriate antibiotics such as ampicillin or kanamycin. Here, single colonies of Q $\beta$  are added to a starter culture (varying in volume from 3-10 mL), and the mixture is incubated at 37°C and 0% relative humidity under shaking conditions for 12 h. The starter culture is then inoculated in a 2 L volume of either LB or SOB and placed in the incubator at 37°C and 0% relative under shaking conditions for 3-5 h. Once the culture reaches an OD<sub>600</sub> between 0.9-1.0, protein expression is induced upon the addition of isopropyl  $\beta$ -D-1 thiogalactopyranoside (**IPTG**) at a final concentration of 0.1 mM. Protein expression is carried out at 37°C, under shaking conditions, for 12 h. Following expression, bacterial cell lysis is done with

the help of either a microfluidizer or via sonication. Finally, cell debris and protein content are separated via centrifugation.

The protein in the supernatant is salted-out from the solution using an excess of ammonium sulfate. The precipitate is then incubated with equal volumes of chloroform/n-butanol, where excess lipids and membrane-bound proteins are removed from the solution. The recovered aqueous layer is then purified via fast-protein liquid chromatography (**FPLC**) or sucrose gradients, depending on the scale of the expression. The first step after purification is concentration determination, where different colorimetric assays such as Bradford, Lowry, or BCA can be employed. Confirmation of Q $\beta$ 's monodispersity is quantitatively measured via dynamic light scattering (**DLS**) and qualitatively via transmission-electron microscopy (**TEM**). The purity of the final product can be assessed through reducing and non-reducing sodium dodecyl sulfate-polyacrylamide (**SDS-PAGE**) and agarose gel electrophoresis.(Brown et al., 2009; Cui et al., 2017)

Q $\beta$  can be modified at lysine residues K2, K13, and K16, as well as the N-terminus; several of these mutants already exist. The VLP also has disulfides at C74 and C80 that can be modified individually, which reduces the thermal stability of the VLP. Another alternative is to employ a cross-linking reaction using dibromomaleimide chemistry optimized by Chen *et al.*, which does not alter the thermal stability of the final VLP.(Chen et al., 2016)

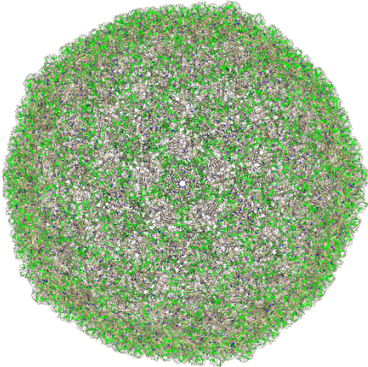
**Table 1. Q $\beta$  examples of bioconjugation reactions. In the figures below, amino acid residues containing carboxylates are shown in green, primary amines in blue, and thiols are shown in yellow.**

VLP	Residue	Incorporated material
	K2, K13, K16, N-terminus	Tn antigen,(Yin et al., 2013) bovine serum albumin,(Hong et al., 2009) fluorescein,(Hong et al., 2009) triple-sulfated ligand,(Mead et al., 2014) AF 488,(Pokorski et al., 2011) AF 568,(Banerjee et al., 2010) human holo-transferrin,(Banerjee et al., 2010) poly(2-oxazoline),(Manzenrieder et al., 2011) PEG-C60,(Steinmetz et al., 2009) oligomannosides,(Astronomo et al., 2010)LacNAc, 50 BPC sialic acid,(Kaltgrad et al., 2008)Gd(DOTA)(Prasuhn et al., 2007)
	M16HPG	Oligomannosides(Astronomo et al., 2010)
	T93AHA	RGD-PEG, biotin(Hovlid et al.)
	C74, C80	Fluorescent PEG, MPEG, polymers and multimeric protein-polymers (Poly(N-isopropylacrylamide[AKNM1]),(Leung et al., 2017; Tao et al., 2009) low and nonimmunogenic antigens (Nicotine[AKNM2])(Maurer et al., 2005)

## P22

Recombinant expression of P22 is commonly achieved using a pET vector containing the scaffold P22 protein and CP. Single colonies of BL21 (DE3) transformed cells are grown using LB media supplemented with ampicillin (50 mg/mL) at 37°C under shaking conditions. Induction of protein expression is achieved upon adding IPTG at a concentration of 0.3 mM final volume. This step is done once cells have reached their mid-log phase (OD<sub>600</sub> of 0.6-0.7). Protein expression is carried out for 4 h, and cells are harvested via centrifugation at 4,500 ×g. Cells are then resuspended in PBS and stored at -80°C. The cell suspension is then thawed and diluted in 5-10 mL g<sup>-1</sup> of pellet in lysis buffer consisting of 100 mM sodium chloride and 50 mM sodium phosphate, pH 7. The mixture is incubated with RNase, DNase, and lysozyme, followed by cell lysis via sonication. Debris is removed by centrifugation, and the resulting supernatant is purified through 35% sucrose cushions. Pelleted P22 capsids are then further purified through FPLC. Fractions containing intact P22 capsids are concentrated using spin-filters of appropriate molecular-weight cut-off (**MWCO**) and analyzed under SDS, agarose, and TEM.(McCoy and Douglas, 2018; Patterson et al., 2012; Schwarz et al., 2015)

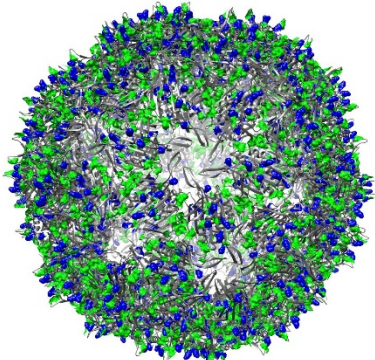
**Table 2. P22 examples of bioconjugation reactions.**

VLP	Residue	Incorporated material
 <p><b>P22</b></p>	S39C	Poly(2-aminoethyl methacrylate),(Lucon et al., 2012b) poly(tris(hydroxymethyl)methacrylamide)(Lucon et al., 2013)
	K110C	Streptavidin(Kang et al., 2010)
	K118C	Poly(tris(hydroxymethyl) methacrylamide),(Lucon et al., 2013) Gd(III)-DTPA-DAA,(Qazi et al., 2013) Gd(III)-DOTA, Gd(III)-DTPA,(Min et al., 2013) streptavidin(Kang et al., 2010)
	V119C	Streptavidin(Kang et al., 2010)
	S133C	Gd(III)-DOTA, Gd(III)-DTPA(Min et al., 2013)
	C-terminal LPTEG tag	Polyglycine GFP, polyglycine hemagglutinin head(Patterson et al., 2017)
	C-terminal SpyTag	EGFRAfb, HER2Afb,(Kim et al., 2019) hemagglutinin head(Sharma and Douglas, 2020)
	C-terminal Cysteine tag	Fluorescein-5-maleimide(Servid et al., 2013)

## MS2

Bacteriophage MS2 is recombinantly produced using a pBAD plasmid.(Robinson et al., 2020) Transformed single colonies are added to LB media supplemented with appropriate antibiotics (e.g., 50 µg/mL ampicillin) and subsequently induced with arabinose. Bacterial cells are collected via centrifugation and frozen at -80°C. For protein isolation, pellets are thawed and resuspended in 20 mM taurine buffer, pH 9.0 consisting of 6.5 mM DTT, 6 mM MgCl<sub>2</sub>, and 10 µg/mL of DNase and Rnase. Incubation in taurine buffer is followed by sonication and collection of cells via centrifugation. Supernatants are purified through Sephadex and then through FPLC. Final purified products are concentrated using 100 kDa MWCO spin filters and characterized through size exclusion chromatography (**SEC**), DLS, SDS-PAGE, agarose, and TEM.(Biela et al., 2022; Plevka et al., 2008)

**Table 3. MS2 examples of bioconjugation reactions.**

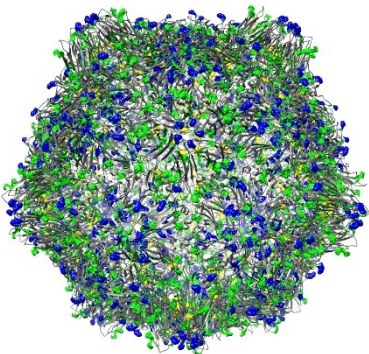
VLP	Residue	Incorporated Material
<p><b>MS2</b></p> 	Y85	Diazonium salt,(Hooker et al., 2004) FAM-SE,(Kovacs et al., 2007) [ <sup>18</sup> F]-benzaldehyde,(Hooker et al., 2008) Gd(III)complex(Datta et al., 2008)
		Gold NPs(Capehart et al., 2014)
	T19pAF	AF488, DNA,(Capehart et al., 2013) DNA aptamers,(Tong et al., 2009) fibrin,(Obermeyer et al., 2014) peptides,(Carrico et al., 2008) PEG,(Farkas et al., 2013) porphyrin(Stephanopoulos et al., 2009)
		DNA(EI Muslemany et al., 2014)
	N87C	AF 488, AF 680,(Obermeyer et al., 2014) DOTA,(Farkas et al., 2013) AF 350, Oregon Green 488,(Stephanopoulos et al., 2009) Gd(III) complex,(Garimella et al., 2011) Taxol,(Wu et al., 2009) Small peptides (α-endorphin)(Lobba et al., 2020)
	K106, K113, N-terminus	PEG(Kovacs et al., 2007) TREN-bis-HOPO-TAM ligand(Datta et al., 2008)

### CPMV

CPMV plant virus is expressed in black-eyed peas (*Vigna unguiculata*). Plant leaves are inoculated with 100 ng/µL CPMV solution in 0.1 M potassium phosphate buffer (pH 7.0) and incubated for 18-20 days.(Wen et al., 2012) The infected leaves are mixed and homogenized with 0.1 M phosphate buffer (pH 7.0) in 2 mL/g of leaf tissue followed by centrifugation at 15,000 ×g for 20 mins. The supernatant is stirred with 0.7 vol. of chloroform and n-butanol (1:1) for 1 min and centrifuged again at 10,000 ×g for 5 mins. The clear aqueous phase is extracted and supplemented with PEG 6000 (4% w/v final concentration) and NaCl (0.2 M final concentration). The mixture is stirred at room temperature to dissolve the PEG and NaCl, followed by incubation

for 1 h. The precipitate is collected by centrifugation at 20,000 ×g for 15 mins, and the pellet is resuspended in 0.01 M phosphate buffer (pH 7.0). The mixture is centrifuged to collect the pellet at 10,000 ×g for 15 mins at 4°C. A sucrose gradient is used to layer the suspension, and the virus is pelleted down at 150,000 ×g for 3 h at 4°C. The virus is resuspended in sterile dH<sub>2</sub>O followed by another round of centrifugation at 10,000 ×g for 15 mins at 4°C. The pellet is preserved in phosphate buffer at pH 7.0 to preserve its infectivity if needed. The concentration of the purified virus is determined using UV-Vis spectroscopy and by measuring the OD at 260 nm.(Wang et al., 2019; Wellink, 1998)

**Table 4. CPMV examples of bioconjugation reactions.**

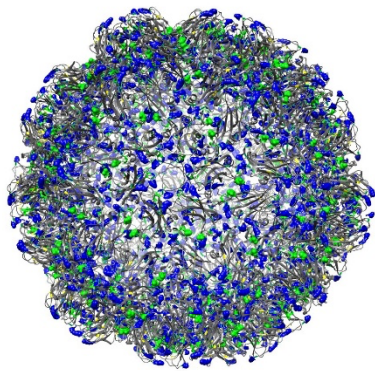
VLP	Residue	Incorporated material
<p><b>CPMV</b></p> 	Lysine	Anti-PD-1 peptide (SNTSESF)(Gautam et al., 2021)
		Bifunctional DBCO-PEG4-NHS ester to enable the chemical conjugation
		Azide-modified antibodies (IgG, hIgG)(Park et al., 2020)
		NHS-Sulfo-Cy5, PEG 2000(Shukla et al., 2020)
		Pluronic F127 coated VNPs
		Peptides for vaccines:
		Myostatin 1
		SARS-CoV-2 peptides
		CH401R (peptides)
		Fluorophore:
Cy5.5 NHS ester		
Therapeutic peptides:		
ApoAI-4FN(Shin et al., 2021)		
Human HLA-A2 restricted peptide antigen NY-ESO-1(Patel et al., 2020)		
Azide alkyne-functionalized generation 3 dendron with Carboxylic group(Wen et al., 2016)		
Complex carbohydrates, peptides, polymers, and proteins(Gupta et al., 2005). polyarginine (R5) cell-penetrating peptides (CPPs)(Wu et al., 2012)		
Lysine and cysteine	CPMV-azides/alkynes with dye alkynes(Wang et al., 2003). Water-solubilized quantum dots of red and green emissions(Portney et al., 2007)	

### CCMV

CCMV virus is expressed and propagated in cowpea leaves.(Bancroft and Hiebert, 1967; Zhao et al., 1995) For the isolation and purification, about 50 – 70 g of the infected cowpea leaves are blended with 2 mL of buffer containing 0.15 M sodium acetate, pH 4.8 per g of plant tissue. One

volume of ice-cold chloroform is then added to the blended mixture while stirring for 10 mins. The resultant mixture is centrifuged at 10,000 ×g for 10 mins. NaCl (0.02 M) and PEG-8000 (8%) are added to the supernatant and stirred for 30 mins. The mixture is centrifuged at 10,000 ×g for 10 mins, and the pellet is resuspended in 20 mL of buffer containing 0.05 M sodium acetate, pH 4.8 in stirring condition for 1 h. The solution is centrifuged at 8,000 ×g for 10 mins, and the supernatant is carefully collected and centrifuged through a 20% sucrose cushion in water at 148,000 ×g for 2 h. The recovered virus pellet is resuspended in 0.05 M sodium acetate, pH 4.8 and characterized through DLS, TEM, agarose, and 10% SDS-PAGE.(Ali and Roossinck, 2007)

**Table 5. CCMV examples of bioconjugation reactions.**

VLP	Residue	Incorporated material
<p><b>CCMV</b></p> 	Lysine	H6/G3 peptides(Chung et al., 2021) M-lycotoxin peptide L17E(Lam and Steinmetz, 2019) DTSSP (3,3' - dithiobis - (sulfosuccinimidylpropionate)(Pretto and van Hest, 2019)
	C-terminus	Oligo-ethylene glycol (OEG) short-chain and an ArgGly-Asp (RGD) peptide(Wu et al., 2014)
	N-terminus	Small molecules and proteins, bearing a C-terminal LPETG-tag(Schoonen et al., 2015)
	Cysteine	24 amino acid peptide(Gillitzer et al., 2002)
		Photosensitizer (Ru(bpy <sub>2</sub> )phen-1A)(Suci et al., 2007)

## TMV

Tobacco (*Nicotiana benthamiana*) plants are used to express and propagate TMV virus.(Geiger et al., 2013; Shukla et al., 2021) Eight week old plants are infected with TMV solution. After two weeks, the leaves are harvested and stored at -80°C until further purification. In the purification process, about 100 g of infected leaves are blended with 300 mL potassium phosphate (KP) buffer with 2-mercaptoethanol (0.2% v/v) at 4°C. The slurry is filtered and centrifuged at 11,000 ×g at 4°C for 20 mins. The supernatant is filtered and mixed with chloroform/1-butanol in a 1:1 ratio at 4°C and incubated for 30 mins. After that, another centrifugation is done at 4,500 ×g for 10 mins. The aqueous phase is then mixed with NaCl (0.2 M), PEG 8000 (8% w/w), and Triton X-100 (1% w/w). The mixture is then stirred on ice for 30 mins and incubated 1 h at 4°C. The mixture is centrifuged again at 22,000 ×g at 4°C for 15 mins. The pellet is collected and resuspended in KP buffer (0.1 M, pH 7.4) and separated on a sucrose gradient at 96,000 ×g for 2 h. After this step,

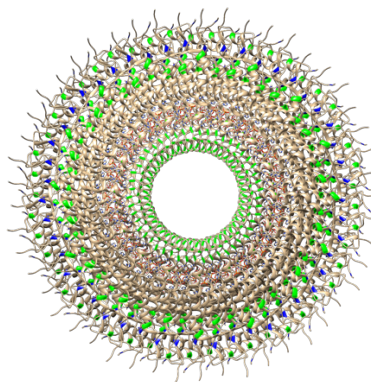
the blue band is extracted with the help of an LED light shining from the bottom of the centrifuge tube. The colloidal suspension obtained from the blue band is further centrifuged at 160,000 ×g for 1.5 h. The resulted TMV pellet is resuspended in KP buffer (0.01 M, pH 7.4) at 4°C until further use.(Lumata et al., 2021)

TMV is typically characterized by TEM using 2% uranyl acetate stain, SDS PAGE, agarose, SEC, and intact protein mass spectrometry. Liquid chromatography-mass spectrometry (**LC-MS**) is another technique used to analyze the integrity of TMV.(Dharmarwardana et al., 2018; Lee et al., 2020)

Native TMV is often modified via diazonium coupling to a surface-exposed tyrosine residue on the outside of the virus. In addition, the inner channel of the virus can be modified at one of several glutamic acid residues. However, diazonium coupling on TMV is tricky; therefore, several mutants of TMV exist that add functional handles that are much easier to use in such bioconjugations.

**Table 6. TMV examples of bioconjugation reactions.**

VLP	Residue	Incorporated material
TMV	Y129	Superoxide sensors,(Lee et al., 2020) high relaxivity MRI contrast agents(Bruckman et al., 2013)
	E97, E106	Texas Red maleimide,(Yi et al., 2005) RBITC,(Liu et al., 2016) FITC, Cy5,(Dharmarwardana et al., 2018) Mitoxantrone,(Lin and Steinmetz, 2018) Phenanthriplatin(Lin and Steinmetz, 2018; Liu et al., 2016; Shukla et al., 2021; Yi et al., 2005)
	T153K	Prostate specific antigen,(Shukla et al., 2021) thrombolytic therapy(Geiger et al., 2013; Shukla et al., 2021)
	S123C	Maleimide PEG conjugation(Koch et al., 2015; Zhou et al., 2013)
	K53, K68	Doxorubicin(Finbloom et al., 2016)
	E50Q, D77N	Disassembly of TMV(Lu et al., 1996)
	T103C	Au nanowires(Zhou et al., 2013)
	MBP TMV	Gold nanoparticles(Love et al., 2015)
	S3C + T153K	Dual functionalization(Wege and Geiger, 2018)

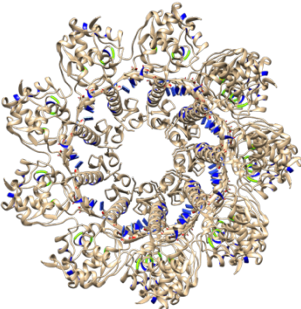


## PVX

PVX virus is usually produced using tobacco (*Nicotiana benthamiana*) plants.(Shukla et al., 2014) First, the PVX-derived plasmid vector is obtained, which consists of a cDNA copy of the PVX viral genome and the 35S promoter. Four-week-old tobacco plant leaves are treated with Celite 545, and three leaves per plant are inoculated with 10 µg of the plasmid. After 14–21 days post-

inoculation, the leaves are harvested and homogenized with ice-cold 0.2 M phosphate buffer in a blender, and the mixture is filtered through a Miracloth followed by centrifugation at 7,800 ×g for 20 mins at 4°C. The supernatant is treated with 1% Triton X-100 and stirred for 1 h at 4°C, followed by centrifugation at 5,500 ×g for 20 mins at 4°C to clarify the mixture. NaCl/PEG is added to the supernatant and centrifuged at 15,000 ×g for 15 mins. The pellet is collected and resuspended in 0.1% 2-mercaptoethanol and 0.5 M urea, followed by centrifugation at 8000 ×g for 30 mins. The supernatant is collected and ultracentrifuged at 160,000 ×g for 3 h to obtain a pellet, which is resuspended in 5 mL buffer and run through a sucrose gradient (10–40%) at 100,000 ×g for 2 h. Finally, the light scattering band is collected and dialyzed against 0.5 M borate buffer, pH 7.8. The virus concentration is determined by UV-Vis spectroscopy and OD at 260 nm. Finally, the virus is characterized by DLS, TEM, SEC, and SDS-PAGE.(Shukla et al., 2013)

**Table 7. PVX examples of bioconjugation reactions.**

VLP	Residue	Incorporated Material
 PVX	Lysine	Oregon Green 488, Biotin, PEG(Steinmetz et al., 2010). Fluorescein(Roder et al., 2019)
	N-terminus	Peptides(Lee et al., 2017)
	Cysteine	Oregon Green 488(Roder et al., 2019)

### Disassembly-Reassembly of VLPs and viruses

Disassembly and reassembly of VLPs is an area of research allowing for the removal of native DNA or RNA and non-covalent loading and encapsulation of cargo.(Stupka and Heddle, 2020) These techniques developed from an increased understanding of the protein capsid unit structures and their native assembly. Advancements in biochemical and biophysical techniques provided insights into which protein interactions helped form and stabilize the capsid. This knowledge was exploited to devise *in vitro* techniques to disassemble the capsid down to their CP units and then recombine them. Foreign material can be incorporated in the second half of the process to help facilitate reassembly, encapsulating said foreign material as the VLP comes together. This method provides a way to incorporate molecules and particles that cannot be conjugated or cannot fit through a pore. Additionally, nucleic acids and other delicate materials can be protected inside these VLPs from harsh environments that could otherwise impact their structural and functional integrity. Below we discuss VLP- or VNP-specific disassembly-reassembly processes and their applicability toward loading the capsid in a ‘supramolecular’ approach. We note that with some VLPs and VNPs, it is also possible to load the capsid “*in vivo*” during expression. For example, the Finn group developed a system to load fluorescent proteins

into Q $\beta$  all in one step during expression.(Rhee et al., 2011) The below methods differ in how the expressed capsid is 'opened up,' and cargo is then encapsulated around the reassembled virus.

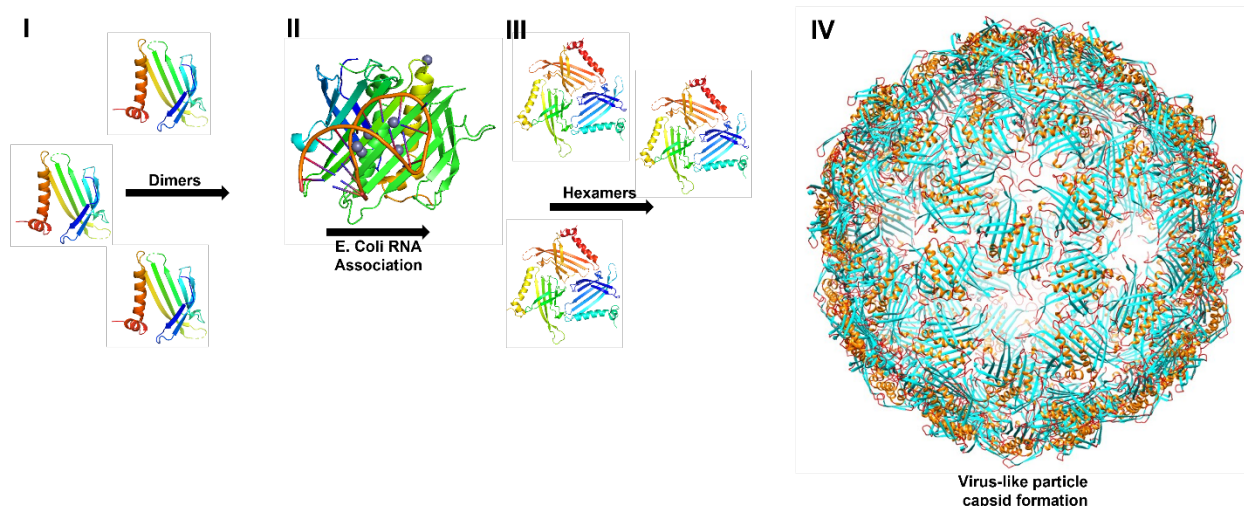


**Figure 5.** Schematic representation of virus-like particle self-assembly.

## Q $\beta$

The assembly of the Q $\beta$  capsid occurs via nonspecific electrostatic interactions between the genomic RNA and the CPs.(Twarock et al., 2018) The cargo-loading process can be achieved both *in vivo* and *in vitro*. *In vivo*—or inside the *E. coli* during/after translation—the helices from multiple CPs interlink into dimers to directly bind to the RNA, encapsulating it in an icosahedral capsid.(Cui et al., 2017) The packaging is promoted by RNA hairpins, which selectively bind to the Q $\beta$  CPs during assembly. Some *in vivo* systems have been optimized to express RNA of interest, around which the CPs assemble and yield the desired encapsulation product.(Fang et al., 2018) This process can be performed *in vitro*—or *post-purification*—with a much larger variety of cargo materials such as DNA, RNA, or even small proteins, as long as the proper conditions are met. *In vitro* assembly is less efficient than *in vivo*, primarily because of the inefficient encapsulation of the genetic material and low yields of reassembled Q $\beta$  with the desired genetic material packed inside.(Fang et al., 2018) However, continuous efforts of researchers in the field have helped develop some successful protocols.

The disassembly of Q $\beta$  *in vitro* starts in a dithiothreitol (DTT)-rich environment to reduce the disulfide bonds. The disassembly buffer also contains a high salt concentration to disrupt the interactions between CPs by decreasing the propensity for CP-CP hydrogen bonding interactions. After incubating Q $\beta$  in the disassembly buffer, disassembled and intact capsids are separated from the solution by centrifugation. Extracted RNA is precipitated with a Lewis base such as MgCl<sub>2</sub>. The Q $\beta$  is then reassembled in a solution containing a new "guest" material to be encapsulated in an appropriate buffer of interest.(Cui et al., 2017) Purification steps to get rid of the excess salts following disassembly often include dialysis and/or running the system through a Sephadex, Sepharose, or Sephacryl column.(C. Gomes et al., 2019)

Herbert *et al.* optimized the disassembly conditions and found that incubating Q $\beta$  in 10 mM DTT, 20 mM Tris-HCl, 6 M urea, and 50 mM NaCl for 5 h at 4°C would induce complete disassembly.(Fang et al., 2018; Herbert et al., 2020) The group then encapsulated smURFP—a small ultra-red fluorescent protein—into the Q $\beta$  capsid to create an *in vivo* imaging tool. Reassembly of the CPs around smURFP was carried out in 50 mM NaCl, and 20 mM Tris-HCl at pH 7.5 and 4°C conditions. It is interesting to note that under these conditions, they afforded the reassembly of the capsid by using a fluorescent protein as the “nucleating center” instead of genetic material. When the same conditions were used without any cargo, the capsid proteins could not reassemble. Since Q $\beta$ 's stability is improved by the disulfide bonds between the cysteines in the CPs, it is wise to induce disulfide bond formation with H<sub>2</sub>O<sub>2</sub> again to ensure the cargo does not leave the pores.

To ensure the original RNA inside the Q $\beta$  is eliminated and only cargo of choice remains, the disassembled CPs may be treated with RNAses if required. Using nucleases not only facilitate the elimination of the starting RNA; Storni *et al.* follow up their encapsulation of the DNA-based immunoadjuvant CpG in Q $\beta$  with a DNase incubation to eliminate the unencapsulated DNA while the protein shell protects the encapsulated DNA.(Storni et al., 2004)

## **P22**

In the case of P22, fundamental studies focused on the conformational changes that the CPs undergo to facilitate the exit of SPs and make room for DNA packaging. Based on circular dichroism and Raman spectroscopy, Tuma *et al.* proposed that the assembly of P22 is first initiated by the interactions between the  $\alpha$ -helical SP subunit (gp8) and  $\beta$ -stranded CP subunit (gp5).(Tuma et al., 1996) These interactions drive the reproducibility of the assembly and thermostability of gp8 in helical form. When unbound, gp8 unfolds, and as the equilibrium shifts towards having more unfolded gp8, assembly of gp5 is initiated. Unfolded gp8 becomes available for further assembly of gp5 units, indicating that the SP acts as a catalyst. The process allows the equilibrium steps enough time to incorporate the dsDNA and is assumed to be the event that drives gp8 unfolding. This is because the packaged genome competes for the internal volume and binding sites previously occupied by the SP. When replicated *in vitro*, the authors propose using guanidine hydrochloride or heating to disturb the SP, facilitating the unfolding event.

Disassembly via heat expansion is one of the most straightforward approaches for the breakdown of the P22 procapsid, as it undergoes irreversible morphological changes upon heating. At around 65°C, the capsid's maturation occurs where its size increases from 58 to 64 nm, with the expansion helping release the SPs. Upon further heating to 75°C, the capsid expands more, and twelve gp5 subunits on the protein shell are irreversibly released, creating 10 nm “holes” in the capsid, an assembly referred to as the “wiffleball” assembly.(Putri et al., 2015) A standard protocol for this approach is incubating the VLP in NaPO<sub>4</sub> and MgCl<sub>2</sub> and heating till the complete expansion of the procapsid, resulting in the wiffleball conformation. It was found that 50% of the expansion from regular to wiffleball conformation was achieved when heated to 65°C, 100% expansion was achieved at 70°C, and wiffleball conformation was observed upon heating to 75°C.(Morris and Prevelige, 2014)

Modern research continues to seek disassembly methods that can be employed in physiological conditions or within ranges of temperature and pH that are suitable for delicate biomaterials to be encapsulated within these VLPs. Kelly et al. demonstrated the use of ring-opening metathesis polymerization (ROMP) for capsid disassembly.(Kelly et al., 2021) First, the P22His<sub>6</sub>GFP was functionalized on the surface-exposed lysine residues with 5-norbornene-2-carboxylic acid using EDC and sulfo-NHS coupling. Aqua-Met—a ruthenium-based ROMP catalyst—was added for ROMP initiation and subsequent capsid disassembly. This method was compared with the more traditional and previously discussed method of heating till 100% expansion was achieved. The breakdown of the capsid was demonstrated by native gel electrophoresis, TEM and DLS.

Even though disassembly for controlled release of fused proteins (to the SP) has found considerable success, re-assembly of P22 remains a challenge for researchers even today. This is due to the inability of CPs to form the uniform icosahedral structures in the absence of SPs, instead forming complex spirals and closed shells of varying sizes.(Earnshaw and King, 1978) More recent advancements demonstrate the unique applications of reassembly techniques, where the SP and CP are individually purified and combined subsequently. Sharma and Douglas vary the stoichiometric ratios of two variations of SP (wild-type and fusion protein with alcohol dehydrogenase) to act as the center for the reassembly of the purified CPs.(Sharma and Douglas, 2020) The assembled P22s of varying types were studied for their trends in enzymatic activity, which was concluded to have an inverse relationship to the fraction of wild-type SP. Such a system is an example of a finely tuned nanoreactor that can yield a precise amount of enzymatic activity desired for a system.

## MS2

Natural assembly of the MS2 capsid occurs through dimerization of CP monomers into the C/C subunit as shown in **Figure 6**. This is followed by the binding of an RNA hairpin, causing a conformational change in the FG loop region turning the C/C dimers into A/B dimers. The dimers form the icosahedral VLPs through interactions facilitated by the FG loop of 60 A/B dimers and 30 C/C dimers.(Fu and Li, 2016) This assembly method leads to the formation of robust particles causing disassembly to require relatively harsh methods.(Li et al., 2019)

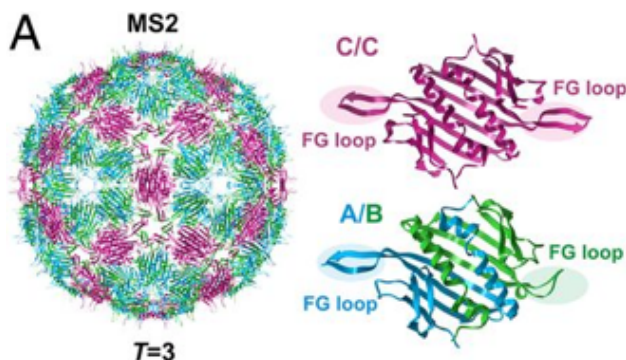


**Figure 6.** Structure of the C/C and A/B subunits and their assembly into the MS2 icosahedral VLP.(Borodavka et al., 2012). Copyright from © 2012 National Academy of Sciences.

In general, wild-type MS2 protein cages disassemble when lowering the pH and then reassemble in the presence of different types of oligonucleotides. The capsid can be disassembled into CP dimers by treatment with 33% to 66% acetic acid while being incubated on ice. Centrifugation is used to remove precipitated RNA and maturase enzymes. The capsid proteins are then desalted using dialysis against an acetic acid gradient or a desalting column. Agarose and native PAGE can be used to confirm disassembly as CP dimers have a molecular weight of 28 kDa. FPLC elution profiles can also be used to confirm the disassembly while UV-Vis spectroscopy can be used to find the concentration of CPs before reassembly.

One of the common methods of reassembly is RNA-driven, in which cargo can be modified with a pac-site RNA.(Ashley et al., 2011) MS2 VLPs reassemble around cargo when CP dimers and RNA-modified cargo are combined in pH 8.5 Tris-HCl buffer at room temperature in a spontaneous process that takes 1 h. This solution can be purified by passing through a Sephadex column to remove free cargo and CP dimers, and/or by running fractions on 1% agarose. This method allows for various types of materials to be encapsulated, such as nanoparticles (e.g., quantum dots), protein toxins (e.g., ricin toxin A-chain), and small-molecule drugs (e.g., doxorubicin).(Ashley et al., 2011) TEM and DLS can be used to confirm the size and structure of the reassembled VLPs. Encapsulation efficiency is commonly done through the disassembly of the particles to release the cargo. UV-Vis is then used to quantify the released RNA, and SDS-PAGE is used for protein quantification; additionally, fluorimetry can be used for fluorescent cargo. Reassembly can also be done by an osmolyte-mediated method where either DNA-modified or charge-modified proteins can induce capsid assembly without the native RNA.(Glasgow et al., 2012) An assembly method driven by capsid concentration using neutral pH buffer was recently developed by Li *et al.* This method can encapsulate negatively charged cargo such as GFP or modified metal nanoparticles through electrostatic interactions. The cargo is mixed with CPs and subsequently dialyzed to increase the concentration to a point where the VLPs self-assemble around the material.(Li et al., 2019)

## **CPMV**

CPMV's genome consists of bipartite, positive-sense ssRNA. Therefore, encapsulation of the viral genome—a crucial step in virus assembly—is challenging as the capsid proteins must preferentially select the genome segments of interest from a high background of cellular mRNA. The two segments of interest are RNA-1 (6kbp) and RNA-2 (3.5 kbp), which are separately encapsidated.(Cheung et al., 2010; Hesketh et al., 2015) RNA-1 contains non-structural genes, whereas RNA-2 consists of sequences encoding the large (L subunit) and small (S subunit) CPs. Not much characterization has been done on the mechanisms underlying the capsid assembly process of CPMV. Though the capsid assembly process of CPMV is not well elucidated in the literature, some suggested mechanisms exist. The C-terminal extension to the S subunit is implicated in capsid assembly and RNA packaging, but understanding their roles have been challenging because the normal maturation of the RNA-filled capsid involves its cleavage and dissociation. Therefore, Hesketh *et al.* have reported detailed characterization and insight on

CPMV biogenesis through high-resolution cryo-EM of a CPMV empty VLP (eVLP) collected on an electron microscope. Cryo-EM reveals the C-terminal extension to the S subunit down to 3.0 Å resolution. Also, the structure for wild-type CPMV contains its larger genomic RNA at 3.4 Å resolution, where the density of the genomic RNA is also resolved. This data, along with the “*de novo*” model built using the high-resolution map obtained from cryo-EM are helpful in understanding which residues are involved in VLP formation and which residues are involved in RNA packaging.(Hesketh et al., 2017)

Usually, the components of CPMV will be resolved as three distinct bands on a sucrose gradient. The top layer contains the artificial top component (AT) – the protein capsid with no detectable RNA, the middle layer has the protein capsid with RNA-2, and the bottom layer has the protein capsid with RNA-1. The common method to remove genomic RNA from CPMV is placing these particles in alkaline/basic conditions. In this process, a mixture of RNA-containing middle and bottom capsids was mixed and incubated in an alkaline buffer containing 0.05 M sodium borate with a pH ranging from 8.5–9.4 at 37°C. When samples were incubated at pH 8.8–9.4, the AT is the only component accumulated in the sucrose gradient because the genomic RNA is degraded at this pH, while the samples incubated at 8.5 showed no accumulation of the AT component. The resulting empty capsid was characterized using ion exchange and SEC.(Ochoa et al., 2006)

Lee *et al.* and Zheng *et al.* have reported a post-purification freeze-drying process to remove RNA from wild-type CPMV producing genome-free CPMV VLPs that retain the capsid structure and function.(Zheng et al., 2019) In this method, they have proven that lyophilization can eject all the encapsulated RNA to form lyo-eCPMV, with almost all the RNA eliminated. The structural integrity of the lyo-eCPMV viral capsid was confirmed through cryo-EM. The limitation of current chemical methods of RNA removal from the capsid is that trace amounts of RNA are still left behind with most techniques. Also, the necessity of fractionation to obtain mostly empty particles and harsh conditions that often lead to denaturation of the capsid over time can be avoided using the lyophilization technique, which was followed by a simple RNase treatment.(Lee et al., 2017)

In most CPMV applications, eCPMV is produced from the agro-infiltrating *Nicotiana benthamiana* leaves with a plasmid construct expressing the precursor of the L- and S-CPs (VP60) and the virus-derived proteinase (24K) required for its processing. The eCPMV particles produced from this method were confirmed to be free from RNA of both the virus and host origin. Here, agrobacterium LBA4404 cultures harboring the binary plasmid were infiltrated into *N. benthamiana* leaves. Infiltrated leaves were harvested six days post infiltration and homogenized in 0.1 M sodium phosphate buffer (pH 7.0). Then the eCPMV was purified further using the same protocol reported for wild-type CPMV.(Wen et al., 2012)

## **CCMV**

CCMV, a 28 nm plant virus, encapsidates four positive sense, ssRNA molecules into three different forms of virions of similar structures. CCMV is considered a model system for viral assembly, as it was the first icosahedral virus to be reassembled *in vitro*. *Virulence is still preserved when assembled from the purified capsid protein dimers and viral RNA of the wild-type CCMV.*(Bancroft and Hiebert, 1967) A remarkable property of reassembled wild-type CCMV is

that it can adopt a wide variety of polymorphic shapes by merely varying the chemical and physical conditions of the reassembly process.(Lavelle et al., 2007)

The wild-type CCMV has proven stable at pH ranging from 3.0–6.0 under low ionic strength (0.5 M) solutions. Therefore, pH above 7.0 and high ionic strength conditions have been used to disassemble the CCMV protein cages. Interestingly, it was found that lowering the ionic strength and pH below 5.0 can reassemble the capsid proteins to form empty CCMV particles of similar structure without the viral RNA genome.(Fox et al., 1998) The disassembly conditions include 0.9 M NaCl, 0.02 M Tris–HCl, 1 mM DTT and 0.5 mM phenylmethylsulfonyl fluoride (PMSF) at pH 7.4. The salts in the disassembly buffer are used to increase its ionic strength, DTT is added to prevent the formation of disulfide bonds, and PMSF is added to inhibit proteases during the disassembly process. Centrifugation of the RNA–protein mixture is carried out at 99,000 ×g for 20 h to pellet down the RNA. The upper ¾ of the supernatant contains the purified protein, which is collected very gently as the RNA pellet is easily disturbed. The concentration of CP solution is usually determined using UV-Vis spectroscopy from the Beer-Lambert law, where  $\epsilon_{280}$  for the CCMV protein monomer equals 23,590 M<sup>-1</sup> cm<sup>-1</sup>.(Fox et al., 1998)

CCMV can be reassembled in the absence of genetic material or other encapsulating cargo; Lavelle *et al.* have reported several reactions under different conditions, varying buffer composition in both ionic strength and pH, whose findings are briefly summarized in Table 8.(Lavelle et al., 2007)

**Table 8:** Different reassembly conditions explored for CCMV.

	pH	Salt concentration	Divalent cation/ chelating agent	Product obtained
1	4.8	High	Mg <sup>2+</sup>	Single layered spherical CCMV-like capsids with 28 nm
2	4.8	High	None/EDTA	CCMV-like particles of 28 nm size. Additional presence of multi-layered, non-uniform spheres.
3	4.8	High, with DTT	Mg <sup>2+</sup>	Both intact and partially assembled CCMV-like particles of similar size
4	4.8	Low	With/out Mg <sup>2+</sup>	Mixture of assembly products (multi-layered and partially assembled)
5	4.8	High	Ba <sup>2+</sup> (poor divalent cation)	Low yield of intact CCMV-like particles

They concluded that the optimal protein-only reassembly of CCMV from its purified CP is most efficient in reassembly buffer conditions of pH 4.8, high salt concentration, and in the presence of divalent cations.(Bancroft and Hiebert, 1967)

CCMV capsid reassembly in the presence of viral RNA genome differs from capsid reassembly with CP only, depending on the CP-CP and CP-RNA interactions and on the order in which the above interactions are “turned on”. To evaluate how the CP-CP and CP-RNA interaction strength affects the overall reassembly process, Garmann *et al.* reported an RNA-mediated assembly protocol for CCMV. The capsid reassembly is achieved by mixing RNA and CP in a 1:6 ratio where CP is in excess at neutral pH. Then the mixture is subjected to subsequent dialysis and equilibration steps. Here, the buffer solution used has a pH of 7.2 and ionic strength of 1.0 M, which minimizes both CP-CP and CP-RNA interactions. The interactions can be subsequently “turned on” by selectively controlling the pH and ionic strength of the buffers used for the dialysis. Depending on the number of dialysis steps used in the assembly process, they can be carried out as a “one-step” or “two-step” reassembly.(Garmann *et al.*, 2019)

## **TMV**

Tobacco mosaic virus is highly stable at room temperature for an extended time.(Geiger *et al.*, 2013) Once the TMV enters the plant cells, the virus disassembles, releases its RNA, and initiates the infection to create new viruses.(Holmes, 1979) The mechanism proposed by Caspar *et al.* includes repulsion between carboxylate-carboxylate functional groups on glutamic and aspartic acids, which resides at the interface between TMV CP subunits. If TMV virus particles are in the extracellular environment, the repulsive forces arising from the negative charges of the carboxylate groups are stabilized by cations like  $\text{Ca}^{2+}$  and  $\text{H}^+$ . When TMV enters the plant cells, the drop in pH, loss of cations, and repulsion between carboxylate groups destabilize the virus and initiate the disassembly process. The first interaction involved in this process is between E50 from the subunit on the axial interface and D77.(Culver, 2002) Subsequent interactions include repulsive forces between E95 and E156 from the neighboring subunit, followed by repulsion between D116 and phosphate groups of the RNA.(Weis *et al.*, 2019)

CPs are weakly bound to the RNA by interactions between the 65 nucleotides located in the 5' end of the RNA, which contains no guanine. Therefore, the first step of destabilizing and disassembling the virions is initiated by removing the CP from the viral RNA. Wilson *et al.* suggest a mechanism that involves attaching ribosomes of the plant cells to the start codon, which get exposed after the removal of the first 23 CPs. The ribosomes bind to the 5' end and start translating the replicase open reading frame leading the removal of CPs. Other components of the proteins are removed through the interaction of the replicase protein with the 3' end. In the same way, RNA transcription gets rid of the other CP subunit proteins with the help of the replicase complex.(Weis *et al.*, 2019)

In the reassembly process, it was found that the CPs are connected through an identical interaction around the RNA subunit. Different conditions can result in different structural assemblies of these helical aggregates. At pH 7.4, the TMV CPs assemble into 20S disks made of 17 molecules per ring. The assembly initiates with the disk, which combines with the single-stranded RNA located 1000 bases after the 3' end. X-ray studies have shown the protein disks to be arranged in a manner where they have gaps that can accommodate the RNA. As shown in **Figure 7**, The nucleation process starts by inserting a hairpin loop between two layers of the subunit. The loop binds to the turn and then opens the base-paired stem-loop, transforming the full disk into a short helix. The disk then entraps the RNA, and more disks are incorporated, elongating the helix. While this helix is elongated, the more it elongates, the more RNA is pulled out of the central cavity. In this fashion, the RNA connects with the subunit proteins, starting the virus' nucleation. The symmetrical rod shape is achieved through non-covalent interactions between subunit proteins.(Zhou et al., 2013)

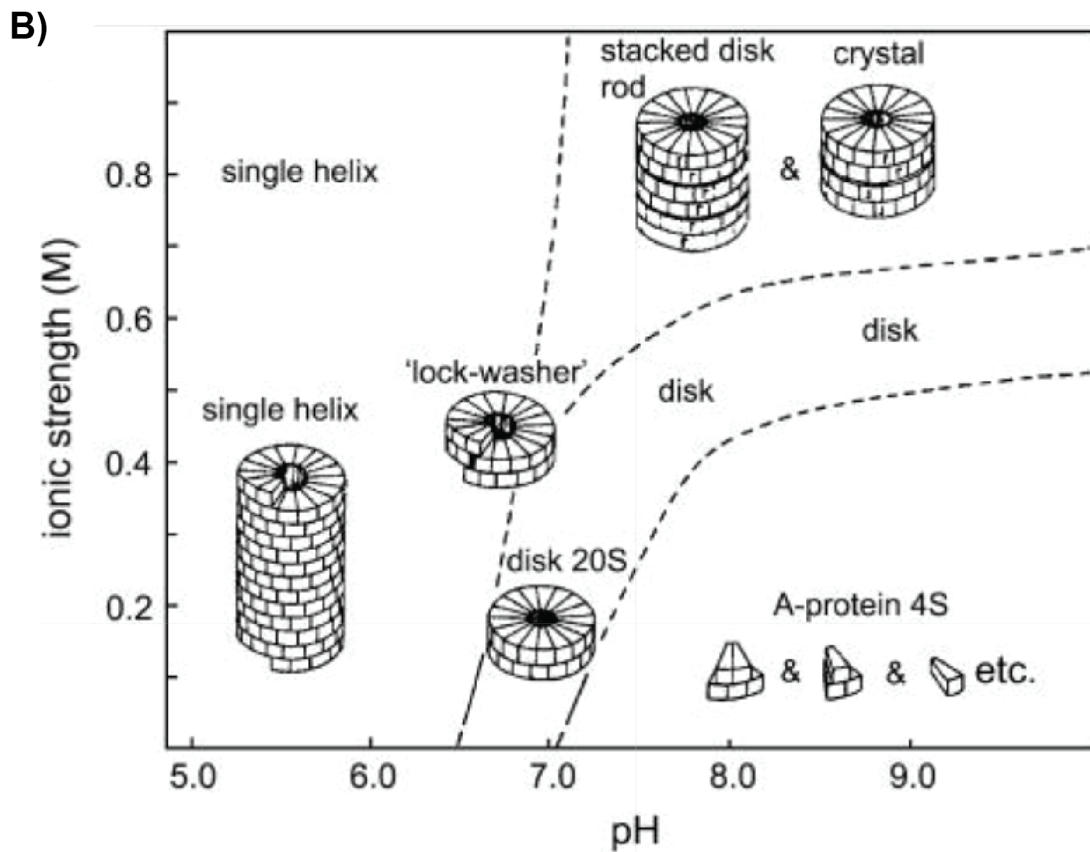
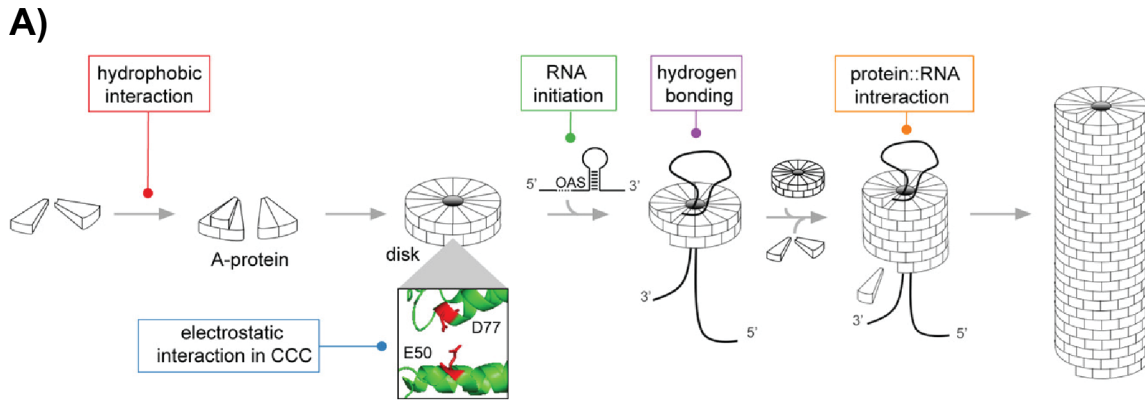


**Figure 7.** A) Process of TMV assembly highlighting various interactions between CPs-CPs and RNA-CPs at different stages of reassembly. (Lee et al., 2021), copyright from © 2020 Wiley-VCH GmbH. B) Stability and states of TMV polymeric protein subunits in aqueous medium in the absence of RNA genome at various ionic strengths at RT, where pH ranging from 5.0-7.0 forms nanorods of TMV. (Kegel and van der Schoot, 2006), copyright from © 2006, Biophysical Society.

Disassembly of the TMV virus in laboratory conditions is done by treating purified TMV with glacial acetic acid for 20 min on ice. RNA is then removed through centrifugation at 20,000  $\times$ g at 4°C.

The supernatant contains the disassembled CPs, which is further purified through dialysis and stored in phosphate buffer at pH 7.2. UV-Vis is used to determine the integrity of the purified CPs, and assembly of these CPs with the RNA cargo is performed simply by co-incubating the constituents at 30°C for 16–20 h in phosphate buffer at pH 7.2.(Lam et al., 2016)

## **PVX**

There are partially overlapping genes in the PVX RNA genome called the triple gene block that consists of TGBp1, TGBp2, and TGBp3, which are responsible for the cell-to-cell movement of PVX. It was found that even though encapsidated RNA of PVX is non-translatable in cell-free translational systems, interaction with TGBp1 will eventually convert it to a completely translatable form.(ATABEKOV et al., 2007) It is reported that the selective binding of TGBp1 to one end of the PVX CP will create a metastable structure by destabilizing the whole helical PVX particle. Even though the binding of this TGBp1 to one end of the PVX plays an essential role in virus disassembly, it was found to be insufficient to achieve complete disassembly. Kiselyova *et al.* demonstrated that co-incubation of TGBp1 with RNase-treated PVX followed by centrifugation at 14,000 ×g or higher resulted in complete disassembly of PVX, as characterized by AFM.(Kiselyova et al., 2003)

Goodman *et al.* have described a straightforward method for the disassembly and reassembly of PVX. Freezing and thawing of purified PVX in 2 M LiCl followed by ultracentrifugation at 117,000 ×g for five hours results in purified CPs free from residual viruses and aggregated CP subunits.(Goodman et al., 1976) In the reassembly process, the viral RNA was combined with protein subunits isolated in LiCl at 22°C in a buffer containing 10 or 20 mM sodium N,N-bis(2-hydroxyethyl) glycine, 10 mM MES, 10 mM sodium cacodylate, 10 mM sodium acetate, 10 mM tris (hydroxymethyl) methylamine or 2 mM sodium phosphate at pH 6.2. The optimum pH of the reassembly buffer was found to be 6.0–6.2. The assembly rate can be measured turbidimetrically, but a more direct indication of rapid assembly can be obtained by pipetting RNA and protein in the appropriate stoichiometric mixtures directly onto 10 mM pH 8.0 sodium EDTA. The reassembly does not occur when the experiment is carried out at 4°C – indicating that PVX reassembly is an entropy-driven reaction. Reassembled PVX has been reported to be less infective than its native counterpart; the ribonuclease-resistant specific infectivity of reassembled PVX varied from 1–14% compared to native PVX as measured by local lesions. The observed low infectivity is due to partial hydrolysis of the RNA after mixing with the CP, which has been previously quantified using PAGE. Dissociated CP subunits do not cross-react with appropriately prepared antiserum made to the virus. However, the reconstituted virus cross-reacted strongly against such antiserum, showing that virus-specific determinant groups were generated upon assembly, which can be used as another test to determine the extent of reassembly when appropriate. Despite the functional differences, structural features observed in the electron micrographs of native and reassembled PVX and their subsequent analysis by optical diffraction do not indicate any distinct differences between both samples.(ATABEKOV et al., 2007)

## Conclusion

VLPs and VNPs are self-assembled nanomaterials that have been extensively investigated in diverse applications. These proteinaceous materials are ideal for imaging and vaccine development investigations, and many groups have exploited this potential. Most VLPs and VNPs are amenable to surface functionalization, disassembly, and reassembly as means to manipulate them. In this review, we have extensively detailed possible methodologies to load cargo and add directing moieties on the surface of these particles, allowing them to be used for various biomedical applications. The architectural diversity of VNPs and VLPs affords researchers numerous options to pick from when tailoring their experimental designs for creating hybrid materials. As the field grows exponentially, the number of VLPs and VNPs currently being tested as immunoadjuvants, vaccines, and imaging agents will continue to flourish and propagate. Finally, we hope to see these emerging technologies transition into clinics soon.

## Declaration of competing interest

The authors have declared that they have no known competing financial interests or personal relationships that could have appeared to influence the work reported in this paper.

## Author contribution

<sup>†</sup> F.C.H and Y.H.W contributed equally.

## CRedit author statement

**Fabian C. Herbert**: Conceptualization; Writing – Original draft; Writing – Review and editing  
**Yalini H. Wijesundara**; Writing – Original draft; Writing – Review and editing; Visualization;  
**Sneha Kumari**; Writing – Original draft; Writing – Review and editing  
**Thomas Howlett**; Writing – Original draft; Writing – Review and editing  
**Shailendra Koirala**; Writing – Original draft  
**Orikeda Trashi**; Writing – Original draft  
**Ikeda Trashi**; Writing – Original draft  
**Noora M. Al-Kharji**; Writing – Original draft.

## Acknowledgements

J.J.G acknowledges National Science Foundation (DMR-2003534) and the Welch Foundation (AT-1989- 20190330).

## References

- Ali, A., Roossinck, M.J., 2007. Rapid and efficient purification of Cowpea chlorotic mottle virus by sucrose cushion ultracentrifugation. *J. Virol. Methods.* 141, 84-86. <https://doi.org/10.1016/j.jviromet.2006.11.038>.
- Arevalo, M.T., Wong, T.M., Ross, T.M., 2016. Expression and Purification of Virus-like Particles for Vaccination. *J. Vis. Exp.* <https://dx.doi.org/10.3791/54041>.
- Ashley, C.E., Carnes, E.C., Phillips, G.K., Durfee, P.N., Buley, M.D., Lino, C.A., Padilla, D.P., Phillips, B., Carter, M.B., Willman, C.L., Brinker, C.J., Caldeira, J.d.C., Chackerian, B., Wharton, W., Peabody, D.S., 2011. Cell-Specific Delivery of Diverse Cargos by Bacteriophage MS2 Virus-like Particles. *ACS Nano.* 5, 5729-5745. <https://doi.org/10.1021/nn201397z>.
- Astronomo, R.D., Kaltgrad, E., Udit, A.K., Wang, S.K., Doores, K.J., Huang, C.Y., Pantophlet, R., Paulson, J.C., Wong, C.H., Finn, M.G., Burton, D.R., 2010. Defining criteria for oligomannose immunogens for HIV using icosahedral virus capsid scaffolds. *Chem. Biol.* 17, 357-370. <https://doi.org/10.1016/j.chembiol.2010.03.012>.
- ATABEKOV, J., DOBROV, E., KARPOVA, O., RODIONOVA, N., 2007. Potato virus X: structure, disassembly and reconstitution. *Mol. Plant Pathol.* 8, 667-675. <https://doi.org/10.1111/j.1364-3703.2007.00420.x>.
- Au - Chen, Z., Au - Detvo, S.T., Au - Pham, E., Au - Gassensmith, J.J., 2018. Making Conjugation-induced Fluorescent PEGylated Virus-like Particles by Dibromomaleimide-disulfide Chemistry. *J. Vis. Exp.* e57712. <https://dx.doi.org/10.3791/57712>.
- Bai, B., Hu, Q., Hu, H., Zhou, P., Shi, Z., Meng, J., Lu, B., Huang, Y., Mao, P., Wang, H., 2008. Virus-like particles of SARS-like coronavirus formed by membrane proteins from different origins demonstrate stimulating activity in human dendritic cells. *PLoS One* 3, e2685. <https://doi.org/10.1371/journal.pone.0002685>.
- Bancroft, J.B., Hiebert, E., 1967. Formation of an infectious nucleoprotein from protein and nucleic acid isolated from a small spherical virus. *Virology* 32, 354-356. [https://doi.org/10.1016/0042-6822\(67\)90284-X](https://doi.org/10.1016/0042-6822(67)90284-X).
- Banerjee, D., Liu, A.P., Voss, N.R., Schmid, S.L., Finn, M.G., 2010. Multivalent display and receptor-mediated endocytosis of transferrin on virus-like particles. *Chembiochem* 11, 1273-1279. <https://doi.org/10.1002/cbic.201000125>.
- Beatty, P.H., Lewis, J.D., 2019. Cowpea mosaic virus nanoparticles for cancer imaging and therapy. *Adv. Drug Deliv. Rev.* 145, 130-144. <https://doi.org/10.1016/j.addr.2019.04.005>.
- Benjamin, C., Brohlin, O., Shahrivarkevishahi, A., Gassensmith, J.J., 2020a. Chapter 11 - Virus like particles: fundamental concepts, biological interactions, and clinical applications, in: Chung, E.J., Leon, L., Rinaldi, C. (Eds.), *Nanoparticles for Biomedical Applications*. Elsevier, pp. 153-174.
- Benjamin, C.E., Chen, Z., Brohlin, O.R., Lee, H., Shahrivarkevishahi, A., Boyd, S., Winkler, D.D., Gassensmith, J.J., 2020b. Using FRET to measure the time it takes for a cell to destroy a virus. *Nanoscale* 12, 9124-9132. <https://doi.org/10.1039/C9NR09816J>.

- Benjamin, C.E., Chen, Z., Kang, P., Wilson, B.A., Li, N., Nielsen, S.O., Qin, Z., Gassensmith, J.J., 2018. Site-Selective Nucleation and Size Control of Gold Nanoparticle Photothermal Antennae on the Pore Structures of a Virus. *J. Am. Chem. Soc.* 140, 17226-17233. <https://doi.org/10.1021/jacs.8b10446>.
- Biabanikhankahdani, R., Ho, K.L., Alitheen, N.B., Tan, W.S., 2018. A Dual Bioconjugated Virus-Like Nanoparticle as a Drug Delivery System and Comparison with a pH-Responsive Delivery System. *Nanomaterials (Basel)* 8. <https://doi.org/10.3390/nano8040236>.
- Biela, A.P., Naskalska, A., Fatehi, F., Twarock, R., Heddle, J.G., 2022. Programmable polymorphism of a virus-like particle. *Commun. Mater.* 3, 7. <https://doi.org/10.1038/s43246-022-00229-3>.
- Borodavka, A., Tuma, R., Stockley Peter, G., 2012. Evidence that viral RNAs have evolved for efficient, two-stage packaging. *Proc. Natl. Acad. Sci.* 109, 15769-15774. <https://doi.org/10.1073/pnas.1204357109>.
- Brea, R.J., Reiriz, C., Granja, J.R., 2010. Towards functional bionanomaterials based on self-assembling cyclic peptide nanotubes. *Chem. Soc. Rev.* 39, 1448-1456. <https://doi.org/10.1039/B805753M>.
- Brown, S.D., Fiedler, J.D., Finn, M.G., 2009. Assembly of Hybrid Bacteriophage Q $\beta$  Virus-like Particles. *Biochemistry* 48, 11155-11157. <https://doi.org/10.1021/bi901306p>.
- Bruckman, M.A., Hern, S., Jiang, K., Flask, C.A., Yu, X., Steinmetz, N.F., 2013. Tobacco mosaic virus rods and spheres as supramolecular high-relaxivity MRI contrast agents. *J. mater. chem. B*, 1, 1482-1490. <https://doi.org/10.1039/C3TB00461A>.
- Butler, P.J.G., 1999. Self-Assembly of Tobacco Mosaic Virus: The Role of an Intermediate Aggregate in Generating Both Specificity and Speed. *Philosophical Transactions: Phil. Trans. R. Soc. Lond. B. Biol. Sci.* 354, 537-550. <https://doi.org/10.1098/rstb.1999.0405>.
- C. Gomes, A., Roesti, E.S., El-Turabi, A., Bachmann, M.F., 2019. Type of RNA Packed in VLPs Impacts IgG Class Switching—Implications for an Influenza Vaccine Design. *Vaccines* 7, 47. <https://doi.org/10.3390/vaccines7020047>.
- Caldeira, J.C., Peabody, D.S., 2011. Thermal Stability of RNA Phage Virus-Like Particles Displaying Foreign Peptides. *J. Nanobiotechnology* 9, 22. <https://doi.org/10.1186/1477-3155-9-22>.
- Capehart, S.L., Coyle, M.P., Glasgow, J.E., Francis, M.B., 2013. Controlled Integration of Gold Nanoparticles and Organic Fluorophores Using Synthetically Modified MS2 Viral Capsids. *J. Am. Chem. Soc.* 135, 3011-3016. <https://doi.org/10.1021/ja3078472>.
- Capehart, S.L., ElSohly, A.M., Obermeyer, A.C., Francis, M.B., 2014. Bioconjugation of gold nanoparticles through the oxidative coupling of ortho-aminophenols and anilines. *Bioconjug. Chem.* 25, 1888-1892. <https://doi.org/10.1021/bc5003746>.
- Carrico, Z.M., Romanini, D.W., Mehl, R.A., Francis, M.B., 2008. Oxidative coupling of peptides to a virus capsid containing unnatural amino acids. *Chem. Commun. (Camb)*, 1205-1207. <https://doi.org/10.1039/b717826c>.

- Casjens, S.R., Grose, J.H., 2016. Contributions of P2- and P22-like prophages to understanding the enormous diversity and abundance of tailed bacteriophages. *Virology* 496, 255-276. <https://doi.org/10.1016%2Fj.virol.2016.05.022>.
- Cervera, L., Gutiérrez-Granados, S., Martínez, M., Blanco, J., Gòdia, F., Segura, M.M., 2013. Generation of HIV-1 Gag VLPs by transient transfection of HEK 293 suspension cell cultures using an optimized animal-derived component free medium. *J. Biotechnol.* 166, 152-165. <https://doi.org/10.1016/j.jbiotec.2013.05.001>.
- Chen, Z., Boyd, S.D., Calvo, J.S., Murray, K.W., Mejia, G.L., Benjamin, C.E., Welch, R.P., Winkler, D.D., Meloni, G., D'Arcy, S., Gassensmith, J.J., 2017. Fluorescent Functionalization across Quaternary Structure in a Virus-like Particle. *Bioconjug. Chem.* 28, 2277-2283. <https://doi.org/10.1021/acs.bioconjchem.7b00305>.
- Chen, Z., Li, N., Chen, L., Lee, J., Gassensmith, J.J., 2016. Dual Functionalized Bacteriophage Q $\beta$  as a Photocaged Drug Carrier. *Small* 12, 4563-4571. <https://doi.org/10.1002/sml.201601053>.
- Cheng, X., Zhu, Z., Liu, Y., Xue, Y., Gao, X., Wang, J., Pei, X., Wan, Q., 2020. Zeolitic Imidazolate Framework-8 Encapsulating Risedronate Synergistically Enhances Osteogenic and Antiresorptive Properties for Bone Regeneration. *ACS Biomater. Sci. Eng.* 6, 2186-2197. <https://doi.org/10.1021/acsbiomaterials.0c00195>.
- Cheung, C.L., Rubinstein, A.I., Peterson, E.J., Chatterji, A., Sabirianov, R.F., Mei, W.-N., Lin, T., Johnson, J.E., DeYoreo, J.J., 2010. Steric and Electrostatic Complementarity in the Assembly of Two-Dimensional Virus Arrays. *Langmuir* 26, 3498-3505. <https://doi.org/10.1021/la903114s>.
- Chi, E.Y., Krishnan, S., Randolph, T.W., Carpenter, J.F., 2003. Physical Stability of Proteins in Aqueous Solution: Mechanism and Driving Forces in Nonnative Protein Aggregation. *Pharm. Res.* 20, 1325-1336. <https://doi.org/10.1023/a:1025771421906>.
- Chung, Y.H., Cai, H., Steinmetz, N.F., 2020. Viral nanoparticles for drug delivery, imaging, immunotherapy, and theranostic applications. *Adv. Drug deliv. Rev.* 156, 214-235. <https://doi.org/10.1016/j.addr.2020.06.024>.
- Chung, Y.H., Park, J., Cai, H., Steinmetz, N.F., 2021. S100A9-Targeted Cowpea Mosaic Virus as a Prophylactic and Therapeutic Immunotherapy against Metastatic Breast Cancer and Melanoma. *Adv. Sci.* 8, e2101796. <https://doi.org/10.1002/adv.202101796>.
- Cui, Z., Gorzelnik, K.V., Chang, J.-Y., Langlais, C., Jakana, J., Young, R., Zhang, J., 2017. Structures of Q $\beta$  virions, virus-like particles, and the Q $\beta$ -MurA complex reveal internal coat proteins and the mechanism of host lysis. *Proc. Natl. Acad. Sci.* 114, 11697-11702. <https://doi.org/10.1073%2Fpnas.1707102114>.
- Culver, J.N., 2002. TOBACCO MOSAIC VIRUS ASSEMBLY AND DISASSEMBLY: Determinants in Pathogenicity and Resistance. *Annu. Rev. Phytopathol.* 40, 287-308. <https://doi.org/10.1146/annurev.phyto.40.120301.102400>.
- Datta, A., Hooker, J.M., Botta, M., Francis, M.B., Aime, S., Raymond, K.N., 2008. High relaxivity gadolinium hydroxypyridonate-viral capsid conjugates: nanosized MRI contrast agents. *J. Am. Chem. Soc.* 130, 2546-2552. <https://doi.org/10.1021/ja0765363>.

de Ruiter, M.V., van der Hee, R.M., Driessen, A.J.M., Keurhorst, E.D., Hamid, M., Cornelissen, J., 2019. Polymorphic assembly of virus-capsid proteins around DNA and the cellular uptake of the resulting particles. *J. Control. Release* 307, 342-354. <https://doi.org/10.1016/j.jconrel.2019.06.019>.

Dharmarwardana, M., Martins, A.F., Chen, Z., Palacios, P.M., Nowak, C.M., Welch, R.P., Li, S., Luzuriaga, M.A., Bleris, L., Pierce, B.S., Sherry, A.D., Gassensmith, J.J., 2018. Nitroxyl Modified Tobacco Mosaic Virus as a Metal-Free High-Relaxivity MRI and EPR Active Superoxide Sensor. *Mol. Pharm.* 15, 2973-2983. <https://doi.org/10.1021%2Facs.molpharmaceut.8b00262>.

Díaz-Caballero, M., Navarro, S., Nuez-Martínez, M., Peccati, F., Rodríguez-Santiago, L., Sodupe, M., Teixidor, F., Ventura, S., 2021. pH-Responsive Self-Assembly of Amyloid Fibrils for Dual Hydrolase-Oxidase Reactions. *ACS Catalysis* 11, 595-607. <https://doi.org/10.1021/acscatal.0c03093>.

Durham, A.C.H., Finch, J.T., Klug, A., 1971. States of Aggregation of Tobacco Mosaic Virus Protein. *Nature New Biol.* 229, 37-42. <https://doi.org/10.1038/newbio229037a0>.

Earnshaw, W., King, J., 1978. Structure of phage P22 coat protein aggregates formed in the absence of the scaffolding protein. *J. Mol. Biol.* 126, 721-747. [https://doi.org/10.1016/0022-2836\(78\)90017-7](https://doi.org/10.1016/0022-2836(78)90017-7).

El Muslemany, K.M., Twite, A.A., ElSohly, A.M., Obermeyer, A.C., Mathies, R.A., Francis, M.B., 2014. Photoactivated Bioconjugation Between ortho-Azidophenols and Anilines: A Facile Approach to Biomolecular Photopatterning. *J. Am. Chem. Soc.* 136, 12600-12606. <https://doi.org/10.1021/ja503056x>.

Fang, P.-Y., Bowman, J.C., Gómez Ramos, Lizzette M., Hsiao, C., Williams, L.D., 2018. RNA: packaged and protected by VLPs. *RSC Advances* 8, 21399-21406. <https://doi.org/10.1039/C8RA02084A>.

Farkas, K., Walker, D.I., Adriaenssens, E.M., McDonald, J.E., Hillary, L.S., Malham, S.K., Jones, D.L., 2020. Viral indicators for tracking domestic wastewater contamination in the aquatic environment. *Water Res.* 181, 115926. <https://doi.org/10.1016%2Fj.watres.2020.115926>.

Farkas, M.E., Aanei, I.L., Behrens, C.R., Tong, G.J., Murphy, S.T., O'Neil, J.P., Francis, M.B., 2013. PET Imaging and biodistribution of chemically modified bacteriophage MS2. *Mol. Pharm.* 10, 69-76. <https://doi.org/10.1021/mp3003754>.

Felice, B., Prabhakaran, M.P., Rodríguez, A.P., Ramakrishna, S., 2014. Drug delivery vehicles on a nano-engineering perspective. *Mater. Sci. Eng. C* 41, 178-195. <https://doi.org/10.1016/j.msec.2014.04.049>.

Finbloom, J.A., Han, K., Aanei, I.L., Hartman, E.C., Finley, D.T., Dedeo, M.T., Fishman, M., Downing, K.H., Francis, M.B., 2016. Stable Disk Assemblies of a Tobacco Mosaic Virus Mutant as Nanoscale Scaffolds for Applications in Drug Delivery. *Bioconjug. Chem.* 27, 2480-2485. <https://doi.org/10.1021/acs.bioconjchem.6b00424>.

Fontana, D., Kratje, R., Etcheverrigaray, M., Prieto, C., 2015. Immunogenic virus-like particles continuously expressed in mammalian cells as a veterinary rabies vaccine candidate. *Vaccine* 33, 4238-4246. <https://doi.org/10.1016/j.vaccine.2015.03.088>.

Fox, J.M., Wang, G., Speir, J.A., Olson, N.H., Johnson, J.E., Baker, T.S., Young, M.J., 1998. Comparison of the Native CCMV Virion within VitroAssembled CCMV Virions by Cryoelectron Microscopy and Image Reconstruction. *Virology* 244, 212-218. <https://doi.org/10.1006/viro.1998.9107>.

Fu, Y., Li, J., 2016. A novel delivery platform based on Bacteriophage MS2 virus-like particles. *Virus Res.* 211, 9-16. <https://doi.org/10.1016%2Fj.virusres.2015.08.022>.

Fuenmayor, J., Gòdia, F., Cervera, L., 2017. Production of virus-like particles for vaccines. *New Biotechnol.* 39, 174-180. <https://doi.org/10.1016/j.nbt.2017.07.010>.

Furiga, A., Pierre, G., Glories, M., Aimar, P., Roques, C., Causserand, C., Berge, M., 2011. Effects of ionic strength on bacteriophage MS2 behavior and their implications for the assessment of virus retention by ultrafiltration membranes. *Appl. Environ. Microbiol.* 77, 229-236. <https://doi.org/10.1128/aem.01075-10>.

Garimella, P.D., Datta, A., Romanini, D.W., Raymond, K.N., Francis, M.B., 2011. Multivalent, high-relaxivity MRI contrast agents using rigid cysteine-reactive gadolinium complexes. *J. Am. Chem. Soc.* 133, 14704-14709. <https://doi.org/10.1021/ja204516p>.

Garmann, R.F., Goldfain, A.M., Manoharan, V.N., 2019. Measurements of the self-assembly kinetics of individual viral capsids around their RNA genome. *Proc. Natl. Acad. Sci.* 116, 22485-22490. <https://doi.org/10.1073/pnas.1909223116>.

Gautam, A., Beiss, V., Wang, C., Wang, L., Steinmetz, N.F., 2021. Plant Viral Nanoparticle Conjugated with Anti-PD-1 Peptide for Ovarian Cancer Immunotherapy. *Int. J. Mol. Sci.* 22. <https://doi.org/10.3390%2Fijms22189733>.

Geiger, F.C., Eber, F.J., Eiben, S., Mueller, A., Jeske, H., Spatz, J.P., Wege, C., 2013. TMV nanorods with programmed longitudinal domains of differently addressable coat proteins. *Nanoscale* 5, 3808-3816. <https://doi.org/10.1039/C3NR33724C>.

Geitner, A.-J., Schmid, F.X., 2012. Combination of the Human Prolyl Isomerase FKBP12 with Unrelated Chaperone Domains Leads to Chimeric Folding Enzymes with High Activity. *J. Mol. Biol.* 420, 335-349. <https://doi.org/10.1016/j.jmb.2012.04.018>.

George, A., Shah, P.A., Shrivastav, P.S., 2019. Natural biodegradable polymers based nano-formulations for drug delivery: A review. *Int. J. Pharm.* 561, 244-264. <https://doi.org/10.1016/j.ijpharm.2019.03.011>.

Gillitzer, E., Willits, D., Young, M., Douglas, T., 2002. Chemical modification of a viral cage for multivalent presentation. *Chem. Commun.* 2390-2391. <https://doi.org/10.1039/B207853H>.

Glasgow, J.E., Capehart, S.L., Francis, M.B., Tullman-Ercek, D., 2012. Osmolyte-Mediated Encapsulation of Proteins inside MS2 Viral Capsids. *ACS Nano* 6, 8658-8664. <https://doi.org/10.1021/nn302183h>.

Goodman, R.M., McDonald, J.G., Horne, R.W., Bancroft, J.B., 1976. Assembly of Flexuous Plant Viruses and Their Proteins. *Philos. Trans. R. Soc. Lond. B. Biol. Sci.* 276, 173-179. <https://doi.org/10.1098/rstb.1976.0108>.

Goulet, M.C., Gaudreau, L., Gagné, M., Maltais, A.M., Laliberté, A.C., Éthier, G., Bechtold, N., Martel, M., D'Aoust, M.A., Gosselin, A., Pepin, S., Michaud, D., 2019. Production of Biopharmaceuticals in *Nicotiana benthamiana*—Axillary Stem Growth as a Key Determinant of Total Protein Yield. *Front. Plant Sci.* 10, 735. <https://doi.org/10.3389/fpls.2019.00735>.

Greco, R., Michel, M., Guetard, D., Cervantes-Gonzalez, M., Pelucchi, N., Wain-Hobson, S., Sala, F., Sala, M., 2007. Production of recombinant HIV-1/HBV virus-like particles in *Nicotiana tabacum* and *Arabidopsis thaliana* plants for a bivalent plant-based vaccine. *Vaccine* 25, 8228-8240. <https://doi.org/10.1016/j.vaccine.2007.09.061>.

Grinzato, A., Kandiah, E., Lico, C., Betti, C., Baschieri, S., Zanotti, G., 2020. Atomic structure of potato virus X, the prototype of the Alphaflexiviridae family. *Nat. Chem. Biol.* 16, 564-569. <https://doi.org/10.1038/s41589-020-0502-4>.

Gupta, S.S., Kuzelka, J., Singh, P., Lewis, W.G., Manchester, M., Finn, M.G., 2005. Accelerated Bioorthogonal Conjugation: A Practical Method for the Ligation of Diverse Functional Molecules to a Polyvalent Virus Scaffold. *Bioconjug. Chem.* 16, 1572-1579. <https://doi.org/10.1021/bc050147l>.

Hagan, M.F., 2014. Modeling Viral Capsid Assembly. *Adv. Chem. Phys.* 155, 1-68. <https://doi.org/10.1002/9781118755815.ch01>.

Hagan, M.F., Elrad, O.M., 2010. Understanding the concentration dependence of viral capsid assembly kinetics—the origin of the lag time and identifying the critical nucleus size. *Biophys. J.* 98, 1065-1074. <https://doi.org/10.1016/j.bpj.2009.11.023>.

Hashemi, K., Ghahramani Seno, M.M., Ahmadian, M.R., Malaekheh-Nikouei, B., Bassami, M.R., Dehghani, H., Afkhami-Goli, A., 2021. Optimizing the synthesis and purification of MS2 virus like particles. *Sci. Rep.* 11, 19851. <https://doi.org/10.1038/s41598-022-12923-w>.

Hema, M., Vishnu Vardhan, G.P., Savithri, H.S., Murthy, M.R.N., 2019. Chapter 6 - Emerging Trends in the Development of Plant Virus-Based Nanoparticles and Their Biomedical Applications, in: Buddolla, V. (Ed.), *Recent Developments in Applied Microbiology and Biochemistry*. Academic Press, Boston, pp. 61-82. <https://doi.org/10.1016/B978-0-12-816328-3.09988-8>.

Herbert, F.C., Brohlin, O.R., Galbraith, T., Benjamin, C., Reyes, C.A., Luzuriaga, M.A., Shahrivarkevishahi, A., Gassensmith, J.J., 2020. Supramolecular Encapsulation of Small-Ultrared Fluorescent Proteins in Virus-Like Nanoparticles for Noninvasive In Vivo Imaging Agents. *Bioconjug. Chem.* 31, 1529-1536. <https://doi.org/10.1021/acs.bioconjchem.0c00190>.

Hermanson, G.T., 2013. Chapter 2 - Functional Targets for Bioconjugation, in: Hermanson, G.T. (Ed.), *Bioconjugate Techniques (Third Edition)*. Academic Press, Boston, pp. 127-228. <https://doi.org/10.1016/B978-0-12-382239-0.00002-9>.

Hesketh, E.L., Meshcheriakova, Y., Dent, K.C., Saxena, P., Thompson, R.F., Cockburn, J.J., Lomonosoff, G.P., Ranson, N.A., 2015. Mechanisms of assembly and genome packaging

in an RNA virus revealed by high-resolution cryo-EM. *Nat. Commun.* 6, 10113.  
<https://doi.org/10.1038/ncomms10113>.

Hesketh, E.L., Meshcheriakova, Y., Thompson, R.F., Lomonosoff, G.P., Ranson, N.A., 2017. The structures of a naturally empty cowpea mosaic virus particle and its genome-containing counterpart by cryo-electron microscopy. *Sci. Rep.* 7, 539.  
<https://doi.org/10.1038/s41598-017-00533-w>.

Holmes, K.C., 1979. Protein-RNA interactions during TMV assembly. *J. Supramol. Struct.* 12, 305-320. <https://doi.org/10.1002/jss.400120304>.

Hong, V., Presolski, S.I., Ma, C., Finn, M.G., 2009. Analysis and optimization of copper-catalyzed azide-alkyne cycloaddition for bioconjugation. *Angew. Chem. Int. Ed. Engl.* 48, 9879-9883. <https://doi.org/10.1002/anie.200905087>.

Hooker, J.M., Kovacs, E.W., Francis, M.B., 2004. Interior Surface Modification of Bacteriophage MS2. *J. Am. Chem. Soc.* 126, 3718-3719. <https://doi.org/10.1021/ja031790q>.

Hooker, J.M., O'Neil, J.P., Romanini, D.W., Taylor, S.E., Francis, M.B., 2008. Genome-free viral capsids as carriers for positron emission tomography radiolabels. *Mol. Imaging Biol.* 10, 182-191. <https://doi.org/10.1007/s11307-008-0136-5>.

Hovlid, M.L., Lau J.L., Breitenkamp, K., Higginson, C.J., Laufer, B., Manchester, M., Finn, M.G., 2014. Encapsidated atom-transfer radical polymerization in Q $\beta$  virus-like nanoparticles. *ACS Nano* 8, 8003-8014. <https://doi.org/10.1021/nn502043d>.

Jeembaeva, M., Jönsson, B., Castelnovo, M., Evilevitch, A., 2010. DNA heats up: energetics of genome ejection from phage revealed by isothermal titration calorimetry. *J. Mol. Biol.* 395, 1079-1087. <https://doi.org/10.1016/j.jmb.2009.11.069>.

Jeevanandam, J., Pal, K., Danquah, M.K., 2019. Virus-like nanoparticles as a novel delivery tool in gene therapy. *Biochimie* 157, 38-47. <https://doi.org/10.1016/j.biochi.2018.11.001>.

Jiou, J., Chiravuri, K., Gudapati, A., Gassensmith, J.J., 2014. The Chemistry of Confined Spaces. *Current Organic Chemistry* 18, 2002-2009.  
<https://doi.org/10.2174/1385272819666140514005254>.

Kaltgrad, E., O'Reilly, M.K., Liao, L., Han, S., Paulson, J.C., Finn, M.G., 2008. On-Virus Construction of Polyvalent Glycan Ligands for Cell-Surface Receptors. *J. Am. Chem. Soc.* 130, 4578-4579. <https://doi.org/10.1021/ja077801n>.

Kang, S., Uchida, M., O'Neil, A., Li, R., Prevelige, P.E., Douglas, T., 2010. Implementation of P22 Viral Capsids as Nanoplatforms. *Biomacromolecules* 11, 2804-2809.  
<https://doi.org/10.1021/bm100877q>.

Katayama, Y., Kalaj, M., Barcus, K.S., Cohen, S.M., 2019. Self-Assembly of Metal–Organic Framework (MOF) Nanoparticle Monolayers and Free-Standing Multilayers. *J. Am. Chem. Soc.* 141, 20000-20003. <https://doi.org/10.1021/jacs.9b10966>.

Kegel, W.K., van der Schoot, P., 2006. Physical regulation of the self-assembly of tobacco mosaic virus coat protein. *Biophys. J.* 91, 1501-1512.  
<https://doi.org/10.1529%2Fbiophysj.105.072603>.

Kelly, M.P., Napolitano, T., Anand, P., Ho, J.S.K., Jabeen, S., Kuppan, J., Manir, S., Holford, M., 2021. Induced Disassembly of a Virus-like Particle under Physiological Conditions for Venom Peptide Delivery. *Bioconjug. Chem.* 32, 111-120.

<https://doi.org/10.1021/acs.bioconjchem.0c00494>.

Kim, H., Choi, H., Bae, Y., Kang, S., 2019. Development of target-tunable P22 VLP-based delivery nanoplatforms using bacterial superglue. *Biotechnol. Bioeng.* 116, 2843-2851.

<https://doi.org/10.1002/bit.27129>.

Kiselyova, O.I., Yaminsky, I.V., Karpova, O.V., Rodionova, N.P., Kozlovsky, S.V., Arkhipenko, M.V., Atabekov, J.G., 2003. AFM Study of Potato Virus X Disassembly Induced by Movement Protein. *J. Mol. Biol.* 332, 321-325. [https://doi.org/10.1016/s0022-2836\(03\)00835-0](https://doi.org/10.1016/s0022-2836(03)00835-0).

Kluge, J.A., Rabotyagova, O., Leisk, G.G., Kaplan, D.L., 2008. Spider silks and their applications. *Trends Biotechnol.* 26, 244-251. <https://doi.org/10.1016/j.tibtech.2008.02.006>.

Koch, C., Wabbel, K., Eber, F.J., Krolla-Sidenstein, P., Azucena, C., Gliemann, H., Eiben, S., Geiger, F., Wege, C., 2015. Modified TMV Particles as Beneficial Scaffolds to Present Sensor Enzymes. *Front. Plant Sci.* 6, 1137. <https://doi.org/10.3389/fpls.2015.01137>.

Konecny, R., Trylska, J., Tama, F., Zhang, D., Baker, N.A., Brooks, C.L., 3rd, McCammon, J.A., 2006. Electrostatic properties of cowpea chlorotic mottle virus and cucumber mosaic virus capsids. *Biopolymers* 82, 106-120. <https://doi.org/10.1002/bip.20409>.

Kovacs, E.W., Hooker, J.M., Romanini, D.W., Holder, P.G., Berry, K.E., Francis, M.B., 2007. Dual-surface-modified bacteriophage MS2 as an ideal scaffold for a viral capsid-based drug delivery system. *Bioconjug. Chem.* 18, 1140-1147. <https://doi.org/10.1021/bc070006e>.

Kozlovskaya, T.M., Cielēns, I., Dreilinga, D., Dišlers, A., Baumanis, V., Ose, V., Pumpēns, P., 1993. Recombinant RNA phage Q $\beta$  capsid particles synthesized and self-assembled in *Escherichia coli*. *Gene* 137, 133-137. [https://doi.org/10.1016/0378-1119\(93\)90261-Z](https://doi.org/10.1016/0378-1119(93)90261-Z).

Krissanaprasit, A., Key, C.M., Pontula, S., LaBean, T.H., 2021. Self-Assembling Nucleic Acid Nanostructures Functionalized with Aptamers. *Chem. Rev.* 121, 13797-13868. <https://doi.org/10.1021/acs.chemrev.0c01332>.

Kutter, E., 2001. Bacteriophages, in: Brenner, S., Miller, J.H. (Eds.), *Encyclopedia of Genetics*. Academic Press, New York, 179-186. <https://doi.org/10.1006/rwgn.2001.0106>.

Lam, P., Gulati, N.M., Stewart, P.L., Keri, R.A., Steinmetz, N.F., 2016. Bioengineering of Tobacco Mosaic Virus to Create a Non-Infectious Positive Control for Ebola Diagnostic Assays. *Sci. Rep.* 6, 23803. <https://doi.org/10.1038/srep23803>.

Lam, P., Steinmetz, N.F., 2019. Delivery of siRNA therapeutics using cowpea chlorotic mottle virus-like particles. *Biomater. Sci.* 7, 3138-3142. <https://doi.org/10.1039/C9BM00785G>.

Lavelle, L., Michel, J.-P., Gingery, M., 2007. The disassembly, reassembly and stability of CCMV protein capsids. *J. Virol. Methods* 146, 311-316.

<https://doi.org/10.1016/j.jviromet.2007.07.020>.

Le, D.H., Hanamura, R., Pham, D.H., Kato, M., Tirrell, D.A., Okubo, T., Sugawara-Narutaki, A., 2013. Self-assembly of elastin-mimetic double hydrophobic polypeptides.

*Biomacromolecules* 14, 1028-1034. <https://doi.org/10.1021/bm301887m>.

Le, D.T., Müller, K.M., 2021. In Vitro Assembly of Virus-Like Particles and Their Applications. *Life* 11, 334. <https://doi.org/10.3390/life11040334>.

Lee, H., Benjamin, C.E., Nowak, C.M., Tuong, L.H., Welch, R.P., Chen, Z., Dharmawardana, M., Murray, K.W., Bleris, L., D'Arcy, S., Gassensmith, J.J., 2018. Regulating the Uptake of Viral Nanoparticles in Macrophage and Cancer Cells via a pH Switch. *Mol. Pharmaceutics* 15, 2984-2990.

<https://doi.org/10.1021/acs.molpharmaceut.8b00348>.

Lee, H., Shahrivarkevishahi, A., Lumata, J.L., Luzuriaga, M.A., Hagge, L.M., Benjamin, C.E., Brohlin, O.R., Parish, C.R., Firouzi, H.R., Nielsen, S.O., Lumata, L.L., Gassensmith, J.J., 2020. Supramolecular and biomacromolecular enhancement of metal-free magnetic resonance imaging contrast agents. *Chem. Sci.* 11, 2045-2050.

<https://doi.org/10.1039/C9SC05510J>.

Lee, K.L., Murray, A.A., Le, D.H.T., Sheen, M.R., Shukla, S., Commandeur, U., Fiering, S., Steinmetz, N.F., 2017. Combination of Plant Virus Nanoparticle-Based in Situ Vaccination with Chemotherapy Potentiates Antitumor Response. *Nano Lett.* 17, 4019-4028.

<https://doi.org/10.1021/acs.nanolett.7b00107>.

Lee, K.Z., Basnayake Pussepitiyalage, V., Lee, Y.-H., Loesch-Fries, L.S., Harris, M.T., Hemmati, S., Solomon, K.V., 2021. Engineering Tobacco Mosaic Virus and Its Virus-Like Particles for Synthesis of Biotemplated Nanomaterials. *Biotechnology Journal* 16, 2000311.

<https://doi.org/10.1002/biot.202000311>.

Lee, Y.S., 2008. Self-assembly and nanotechnology : a force balance approach / Yoon S. Lee. John Wiley & Sons, Hoboken, N.J. <http://dx.doi.org/10.1002/9780470292525>.

Lemke-Miltner, C.D., Blackwell, S.E., Yin, C., Krug, A.E., Morris, A.J., Krieg, A.M., Weiner, G.J., 2020. Antibody Opsonization of a TLR9 Agonist-Containing Virus-like Particle Enhances In Situ Immunization. *J. Immunol.* 204, 1386-1394.

<https://doi.org/10.4049/jimmunol.1900742>.

Leung, R.L.C., Robinson, M.D.M., Ajabali, A.A.A., Karunanithy, G., Lyons, B., Raj, R., Raoufmoghaddam, S., Mohammed, S., Claridge, T.D.W., Baldwin, A.J., Davis, B.G., 2017. Monitoring the Disassembly of Virus-like Particles by <sup>19</sup>F-NMR. *J. Am. Chem. Soc.* 139, 5277-5280. <https://doi.org/10.1021/jacs.6b11040>.

Levin, A., Hakala, T.A., Schnaider, L., Bernardes, G.J.L., Gazit, E., Knowles, T.P.J., 2020. Biomimetic peptide self-assembly for functional materials. *Nat. Rev. Chem.* 4, 615-634.

<https://doi.org/10.1038/s41570-020-0215-y>.

- Li, L., Xu, C., Zhang, W., Secundo, F., Li, C., Zhang, Z.-P., Zhang, X.-E., Li, F., 2019. Cargo-Compatible Encapsulation in Virus-Based Nanoparticles. *Nano Lett.* 19, 2700-2706. <https://doi.org/10.1021/acs.nanolett.9b00679>.
- Lico, C., Benvenuto, E., Baschieri, S., 2015. The Two-Faced Potato Virus X: From Plant Pathogen to Smart Nanoparticle. *Front. Plant Sci.* 6, 1009. <https://doi.org/10.3389/fpls.2015.01009>
- Liepold, L.O., Revis, J., Allen, M., Oltrogge, L., Young, M., Douglas, T., 2005. Structural transitions in Cowpea chlorotic mottle virus (CCMV). *Phys. Biol.* 2, S166-172. <https://doi.org/10.1088/1478-3975/2/4/s11>.
- Lin, R.D., Steinmetz, N.F., 2018. Tobacco mosaic virus delivery of mitoxantrone for cancer therapy. *Nanoscale* 10, 16307-16313. <https://doi.org/10.1039/c8nr04142c>.
- Lin, T., Johnson, J.E., 2003. Structures of Picorna-Like Plant Viruses: Implications and Applications, *Adv. Virus Res.* 62, 167-239. [https://doi.org/10.1016/s0065-3527\(03\)62004-x](https://doi.org/10.1016/s0065-3527(03)62004-x).
- Liu, J., Dai, S., Wang, M., Hu, Z., Wang, H., Deng, F., 2016. Virus like particle-based vaccines against emerging infectious disease viruses. *Viol. Sin.* 31, 279-287. <https://doi.org/10.1007/s12250-016-3756-y>.
- Lobba, M.J., Fellmann, C., Marmelstein, A.M., Maza, J.C., Kissman, E.N., Robinson, S.A., Staahl, B.T., Urnes, C., Lew, R.J., Mogilevsky, C.S., Doudna, J.A., Francis, M.B., 2020. Site-Specific Bioconjugation through Enzyme-Catalyzed Tyrosine-Cysteine Bond Formation. *ACS Cent. Sci.* 6, 1564-1571. <https://doi.org/10.1021/acscentsci.0c00940>.
- Lomonosoff, G.P., Wege, C., 2018. Chapter Six - TMV Particles: The Journey From Fundamental Studies to Bionanotechnology Applications. *Adv. Virus Res.* 102, 149-176. <https://doi.org/10.1016/bs.aivir.2018.06.003>.
- Love, A., Makarov, V., Sinitsyna, O., Shaw, J., Yaminsky, I., Kalinina, N., Taliansky, M., 2015. A genetically modified tobacco mosaic virus that can produce gold nanoparticles from a metal salt precursor. *Front. Plant Sci.* 6, 984. <https://doi.org/10.3389/fpls.2015.00984>.
- Lu, B., Stubbs, G., Culver, J.N., 1996. Carboxylate Interactions Involved in the Disassembly of Tobacco Mosaic Tobamovirus. *Virology* 225, 11-20. <https://doi.org/10.1006/viro.1996.0570>.
- Lucon, J., Edwards, E., Qazi, S., Uchida, M., Douglas, T., 2013. Atom transfer radical polymerization on the interior of the P22 capsid and incorporation of photocatalytic monomer crosslinks. *Eur. Polym. J.* 49, 2976-2985. <https://doi.org/10.1016/j.eurpolymj.2013.06.010>.
- Lucon, J., Qazi, S., Uchida, M., Bedwell, G.J., LaFrance, B., Prevelige, P.E., Douglas, T., 2012a. Use of the interior cavity of the P22 capsid for site-specific initiation of atom-transfer radical polymerization with high-density cargo loading. *Nat. Chem.* 4, 781-788. <https://doi.org/10.1038/nchem.1442>.
- Lumata, J.L., Ball, D., Shahrivarkevishahi, A., Luzuriaga, M.A., Herbert, F.C., Brohlin, O., Lee, H., Hagge, L.M., D'Arcy, S., Gassensmith, J.J., 2021. Identification and physical characterization of a spontaneous mutation of the tobacco mosaic virus in the laboratory environment. *Sci. Rep.* 11, 15109. <https://doi.org/10.1038/s41598-021-94561-2>.

- Luzuriaga, M.A., Shahrivarkevishahi, A., Herbert, F.C., Wijesundara, Y.H., Gassensmith, J.J., 2021. Biomaterials and nanomaterials for sustained release vaccine delivery. *WIREs Nanomed. Nanobiotechnol.* 13, e1735. <https://doi.org/10.1002/wnan.1735>.
- Maassen, S.J., Huskens, J., Cornelissen, J.J.L.M., 2019. Elucidating the Thermodynamic Driving Forces of Polyanion-Templated Virus-like Particle Assembly. *J. Phys. Chem. B* 123, 9733-9741. <https://doi.org/10.1021/acs.jpcc.9b06258>.
- Manzenrieder, F., Luxenhofer, R., Retzlaff, M., Jordan, R., Finn, M.G., 2011. Stabilization of virus-like particles with poly(2-oxazoline)s. *Angew. Chem., Int. Ed. Engl.* 50, 2601-2605. <https://doi.org/10.1002/ange.201006134>.
- Martí, M., Merwaiss, F., Butković, A., Daròs, J.-A., 2022. Production of Potyvirus-Derived Nanoparticles Decorated with a Nanobody in Biofactory Plants. *Front. Bioeng. Biotechnol.* 10. <https://doi.org/10.3389/fbioe.2022.877363>.
- Mastico, R.A., Talbot, S.J., Stockley, P.G., 1993. Multiple presentation of foreign peptides on the surface of an RNA-free spherical bacteriophage capsid. *J. Gen. Virol.* 74, 541-548. <https://doi.org/10.1099/0022-1317-74-4-541>.
- Maurer, P., Jennings, G.T., Willers, J., Rohner, F., Lindman, Y., Roubicek, K., Renner, W.A., Müller, P., Bachmann, M.F., 2005. A therapeutic vaccine for nicotine dependence: preclinical efficacy, and Phase I safety and immunogenicity. *Eur. J. Immunol.* 35, 2031-2040. <https://doi.org/10.1002/eji.200526285>.
- McCoy, K., Douglas, T., 2018. In Vivo Packaging of Protein Cargo Inside of Virus-Like Particle P22, in: Wege, C., Lomonosoff, G.P. (Eds.), *Virus-Derived Nanoparticles for Advanced Technologies: Methods and Protocols*. Springer New York, New York, NY, pp. 295-302. [https://doi.org/10.1007/978-1-4939-7808-3\\_20](https://doi.org/10.1007/978-1-4939-7808-3_20).
- McManus, J.J., Charbonneau, P., Zaccarelli, E., Asherie, N., 2016. The physics of protein self-assembly. *Curr. Opin. Colloid. Interface. Sci.* 22, 73-79. <https://doi.org/10.1016/j.cocis.2016.02.011>.
- Mead, G., Hiley, M., Ng, T., Fihn, C., Hong, K., Groner, M., Miner, W., Drugan, D., Hollingsworth, W., Udit, A.K., 2014. Directed polyvalent display of sulfated ligands on virus nanoparticles elicits heparin-like anticoagulant activity. *Bioconjug. Chem.* 25, 1444-1452. <https://doi.org/10.1021/bc500200t>.
- Mendes, A.C., Baran, E.T., Reis, R.L., Azevedo, H.S., 2013. Self-assembly in nature: using the principles of nature to create complex nanobiomaterials. *Wiley Interdiscip. Rev. Nanomed. Nanobiotechnol.* 5, 582-612. <https://doi.org/10.1002/wnan.1238>.
- Min, J., Jung, H., Shin, H.-H., Cho, G., Cho, H., Kang, S., 2013. Implementation of P22 Viral Capsids As Intravascular Magnetic Resonance T1 Contrast Conjugates via Site-Selective Attachment of Gd(III)-Chelating Agents. *Biomacromolecules* 14, 2332-2339. <https://doi.org/10.1021/bm400461j>.
- Moore, S.D., Prevelige, P.E., Jr., 2002. A P22 scaffold protein mutation increases the robustness of head assembly in the presence of excess portal protein. *J. Virol.* 76, 10245-10255. <https://doi.org/10.1128/JVI.76.20.10245-10255.2002>.

- Morris, D.S., Prevelige, P.E., 2014. The role of the coat protein A-domain in p22 bacteriophage maturation. *Viruses* 6, 2708-2722. <https://doi.org/10.3390/v6072708>.
- Muller, S., 1999. Chapter 1 - Molecular dissection of protein antigens and the prediction of epitopes, in: Van Regenmortel, M.H.V., Muller, S. (Eds.), *Laboratory Techniques in Biochemistry and Molecular Biology*. Elsevier, pp. 1-78.
- Naskalska, A., Pyrc, K., 2015. Virus Like Particles as Immunogens and Universal Nanocarriers. *Pol. J. Microbiol.* 64, 3-13.
- Nebel, S., Bartoldus, I., Stegmann, T., 1995. Calorimetric detection of influenza virus induced membrane fusion. *Biochemistry* 34, 5705-5711. <https://doi.org/10.1021/bi00017a001>.
- Ng, C.C., Cheng, Y.-L., Pennefather, P.S., 2004. Properties of a self-assembled phospholipid membrane supported on lipobeads. *Biophys. J.* 87, 323-331. <https://doi.org/10.1529/biophysj.103.030627>.
- Niehl, A., Appaix, F., Boscá, S., van der Sanden, B., Nicoud, J.-F., Bolze, F., Heinlein, M., 2016. Fluorescent Tobacco mosaic virus-Derived Bio-Nanoparticles for Intravital Two-Photon Imaging. *Front. Plant Sci.* 6. <https://doi.org/10.3389/fpls.2015.01244>.
- Nitta, S.K., Numata, K., 2013. Biopolymer-Based Nanoparticles for Drug/Gene Delivery and Tissue Engineering. *Int. J. Mol. Sci.* 14, 1629-1654. <https://doi.org/10.3390/ijms14011629>.
- Nooraei, S., Bahrulolum, H., Hoseini, Z.S., Katalani, C., Hajizade, A., Easton, A.J., Ahmadian, G., 2021. Virus-like particles: preparation, immunogenicity and their roles as nanovaccines and drug nanocarriers. *J. Nanobiotechnology* 19, 59. <https://doi.org/10.1186/s12951-021-00806-7>.
- Obermeyer, A.C., Capehart, S.L., Jarman, J.B., Francis, M.B., 2014. Multivalent viral capsids with internal cargo for fibrin imaging. *PLoS One* 9, e100678. <https://doi.org/10.1371/journal.pone.0100678>.
- Ochoa, W.F., Chatterji, A., Lin, T., Johnson, J.E., 2006. Generation and structural analysis of reactive empty particles derived from an icosahedral virus. *Chem. Biol.* 13, 771-778. <https://doi.org/10.1016/j.chembiol.2006.05.014>.
- Park, J., Chariou, P.L., Steinmetz, N.F., 2020. Site-Specific Antibody Conjugation Strategy to Functionalize Virus-Based Nanoparticles. *Bioconjug. Chem.* 31, 1408-1416. <https://doi.org/10.1021/acs.bioconjchem.0c00118>.
- Patel, B.K., Wang, C., Lorens, B., Levine, A.D., Steinmetz, N.F., Shukla, S., 2020. Cowpea Mosaic Virus (CPMV)-Based Cancer Testis Antigen NY-ESO-1 Vaccine Elicits an Antigen-Specific Cytotoxic T Cell Response. *ACS Appl. Bio Mater.* 3, 4179-4187. <https://doi.org/10.1021/acsabm.0c00259>.
- Patterson, D., Schwarz, B., Avera, J., Western, B., Hicks, M., Krugler, P., Terra, M., Uchida, M., McCoy, K., Douglas, T., 2017. Sortase-Mediated Ligation as a Modular Approach for the Covalent Attachment of Proteins to the Exterior of the Bacteriophage P22 Virus-like Particle. *Bioconjug. Chem.* 28, 2114-2124. <https://doi.org/10.1021/acs.bioconjchem.7b00296>.

Patterson, D.P., 2018. Encapsulation of Active Enzymes within Bacteriophage P22 Virus-Like Particles. *Methods Mol. Biol.* 1798, 11-24. [https://doi.org/10.1007/978-1-4939-7893-9\\_2](https://doi.org/10.1007/978-1-4939-7893-9_2).

Patterson, D.P., Schwarz, B., El-Boubbou, K., van der Oost, J., Prevelige, P.E., Douglas, T., 2012. Virus-like particle nanoreactors: programmed encapsulation of the thermostable CelB glycosidase inside the P22 capsid. *Soft Matter* 8, 10158-10166. <https://doi.org/10.1039/C2SM26485D>.

Peabody, D.S., Manifold-Wheeler, B., Medford, A., Jordan, S.K., do Carmo Caldeira, J., Chackerian, B., 2008. Immunogenic display of diverse peptides on virus-like particles of RNA phage MS2. *J. Mol. Biol.* 380, 252-263. <https://doi.org/10.1016/j.jmb.2008.04.049>.

Perlmutter, J.D., Hagan, M.F., 2015. Mechanisms of Virus Assembly. *Annu. Rev. Phys. Chem.* 66, 217-239. <https://doi.org/10.1146/annurev-physchem-040214-121637>.

Petes, T.D., Hereford, L.M., Skryabin, K.G., 1978. Characterization of two types of yeast ribosomal DNA genes. *J. Bacteriology* 134, 295-305. <https://doi.org/10.1128/jb.134.1.295-305.1978>.

Plevka, P., Tars, K., Liljas, L., 2008. Crystal packing of a bacteriophage MS2 coat protein mutant corresponds to octahedral particles. *Protein Sci.* 17, 1731-1739. <https://doi.org/10.1110/ps.036905.108>.

Pochan, D., Scherman, O., 2021. Introduction: Molecular Self-Assembly. *Chemical Reviews* 121, 13699-13700. <https://doi.org/10.1110/ps.036905.108>.

Pokorski, J.K., Breitenkamp, K., Liepold, L.O., Qazi, S., Finn, M.G., 2011. Functional Virus-Based Polymer-Protein Nanoparticles by Atom Transfer Radical Polymerization. *J Am. Chem. Soc.* 133, 9242-9245. <https://doi.org/10.1021/ja203286n>.

Portney, N.G., Tseng, R.J., Destito, G., Strable, E., Yang, Y., Manchester, M., Finn, M., Ozkan, M., 2007. Microscale memory characteristics of virus-quantum dot hybrids. *Appl. Phys. Lett.* 90, 214104. <https://doi.org/10.1063/1.2742787>.

Prasuhn, D.E., Jr., Yeh, R.M., Obenaus, A., Manchester, M., Finn, M.G., 2007. Viral MRI contrast agents: coordination of Gd by native virions and attachment of Gd complexes by azide-alkyne cycloaddition. *Chem. Commun. (Camb)*, 1269-1271. <https://doi.org/10.1039/B615084E>.

Pretto, C., van Hest, J.C.M., 2019. Versatile Reversible Cross-Linking Strategy to Stabilize CCMV Virus Like Particles for Efficient siRNA Delivery. *Bioconjug. Chem.* 30, 3069-3077. <https://doi.org/10.1021/acs.bioconjchem.9b00731>.

Putri, R.M., Cornelissen, J.J., Koay, M.S., 2015. Self-assembled cage-like protein structures. *Chemphyschem* 16, 911-918. <https://doi.org/10.1002/cphc.201402722>.

Qazi, S., Liepold, L.O., Abedin, M.J., Johnson, B., Prevelige, P., Frank, J.A., Douglas, T., 2013. P22 Viral Capsids as Nanocomposite High-Relaxivity MRI Contrast Agents. *Mol. Pharmaceutics* 10, 11-17. <https://doi.org/10.1021/mp300208g>.

Rae, C., Koudelka, K.J., Destito, G., Estrada, M.N., Gonzalez, M.J., Manchester, M., 2008. Chemical addressability of ultraviolet-inactivated viral nanoparticles (VNPs). *PloSone* 3, e3315-e3315. <https://doi.org/10.1371/journal.pone.0003315>.

Rahimzadeh, M., Sadeghizadeh, M., Najafi, F., Arab, S., Mobasheri, H., 2016. Impact of heat shock step on bacterial transformation efficiency. *Molecular biology research communications* 5, 257-261. DOI:10.22099/MBRC.2016.3915

Renner, J.N., Cherry, K.M., Su, R.S., Liu, J.C., 2012. Characterization of resilin-based materials for tissue engineering applications. *Biomacromolecules* 13, 3678-3685. <https://doi.org/10.1021/bm301129b>.

Rhee, J.-K., Hovlid, M., Fiedler, J.D., Brown, S.D., Manzenrieder, F., Kitagishi, H., Nycholat, C., Paulson, J.C., Finn, M.G., 2011. Colorful Virus-like Particles: Fluorescent Protein Packaging by the Q $\beta$  Capsid. *Biomacromolecules* 12, 3977-3981. <https://doi.org/10.1021/bm200983k>.

Robinson, S.A., Hartman, E.C., Ikwuagwu, B.C., Francis, M.B., Tullman-Ercek, D., 2020. Engineering a Virus-like Particle to Display Peptide Insertions Using an Apparent Fitness Landscape. *Biomacromolecules* 21, 4194-4204. <https://doi.org/10.1021/acs.biomac.0c00987>.

Roder, J., Dickmeis, C., Commandeur, U., 2019. Small, Smaller, Nano: New Applications for Potato Virus X in Nanotechnology. *Front. Plant Sci.* 10, 158. <https://doi.org/10.3389/fpls.2019.00158>.

Roldão, A., Mellado, M.C., Castilho, L.R., Carrondo, M.J., Alves, P.M., 2010. Virus-like particles in vaccine development. *Expert Rev Vaccines* 9, 1149-1176. <https://doi.org/10.1586/erv.10.115>.

Rubio, L., Galipienso, L., Ferriol, I., 2020. Detection of Plant Viruses and Disease Management: Relevance of Genetic Diversity and Evolution. *Frontiers in Plant Science* 11. <https://doi.org/10.3389/fpls.2020.01092>.

Sainsbury, F., Cañizares, M.C., Lomonossoff, G.P., 2010. Cowpea mosaic Virus: The Plant Virus-Based Biotechnology Workhorse. *Annual Review of Phytopathology* 48, 437-455. <https://doi.org/10.1586/erv.10.115>.

Salas, M., de Vega, M., 2008. Replication of Bacterial Viruses, in: Mahy, B.W.J., Van Regenmortel, M.H.V. (Eds.), *Encyclopedia of Virology* (Third Edition). Academic Press, Oxford, pp. 399-406.

Saldaña, S., Esquivel Guadarrama, F., Olivera Flores Tde, J., Arias, N., López, S., Arias, C., Ruiz-Medrano, R., Mason, H., Mor, T., Richter, L., Arntzen, C.J., Gómez Lim, M.A., 2006. Production of rotavirus-like particles in tomato (*Lycopersicon esculentum* L.) fruit by expression of capsid proteins VP2 and VP6 and immunological studies. *Viral Immunol* 19, 42-53.

Schmit, J., Whitelam, S., Dill, K., 2010. Competition between counterion entropy and local binding selects dimensionality of charged nanostructures. <https://doi.org/10.1021/acs.chemrev.6b00196>.

Schoonen, L., Pille, J., Borrmann, A., Nolte, R.J., van Hest, J.C., 2015. Sortase A-Mediated N-Terminal Modification of Cowpea Chlorotic Mottle Virus for Highly Efficient Cargo Loading. *Bioconjug Chem* 26, 2429-2434. <https://doi.org/10.1021/acs.bioconjchem.5b00485>.

Schwarz, B., Douglas, T., 2015. Development of virus-like particles for diagnostic and prophylactic biomedical applications. *Wiley interdiscip. Rev. Nanomed. Nanobiotechnol.* 7, 722-735. <https://doi.org/10.1002/wnan.1336>.

Schwarz, B., Madden, P., Avera, J., Gordon, B., Larson, K., Miettinen, H.M., Uchida, M., LaFrance, B., Basu, G., Rynda-Apelle, A., Douglas, T., 2015. Symmetry Controlled, Genetic Presentation of Bioactive Proteins on the P22 Virus-like Particle Using an External Decoration Protein. *ACS Nano* 9, 9134-9147. <https://doi.org/10.1021/acs.nano.5b03360>.

Servid, A., Jordan, P., O'Neil, A., Prevelige, P., Douglas, T., 2013. Location of the Bacteriophage P22 Coat Protein C-Terminus Provides Opportunities for the Design of Capsid-Based Materials. *Biomacromolecules* 14, 2989-2995. <https://doi.org/10.1021/bm400796c>.

Seul, A., Müller, J.J., Andres, D., Stettner, E., Heinemann, U., Seckler, R., 2014. Bacteriophage P22 tailspike: structure of the complete protein and function of the interdomain linker. *Acta. Crystallogr. D. Biol. Crystallogr.* 70, 1336-1345. <https://doi.org/10.1107/S1399004714002685>.

Shahrivarkevishahi, A., Hagge, L.M., Brohlin, O.R., Kumari, S., Ehrman, R., Benjamin, C., Gassensmith, J.J., 2022. Virus-like particles: a self-assembled toolbox for cancer therapy. *Mater. Today Chem.* 24, 100808. <https://doi.org/10.1016/j.mtchem.2022.100808>.

Shahrivarkevishahi, A., Luzuriaga, M.A., Herbert, F.C., Tumac, A.C., Brohlin, O.R., Wijesundara, Y.H., Adlooru, A.V., Benjamin, C., Lee, H., Parsamian, P., Gadhvi, J., De Nisco, N.J., Gassensmith, J.J., 2021. Photothermal Phage: A Virus-Based Photothermal Therapeutic Agent. *J Am Chem Soc.* 143, 16428-16438. <https://doi.org/10.1021/jacs.1c05090>.

Sharma, J., Douglas, T., 2020. Tuning the catalytic properties of P22 nanoreactors through compositional control. *Nanoscale* 12, 336-346. <https://doi.org/10.1039/C9NR08348K>.

Sharma, J., Uchida, M., Miettinen, H.M., Douglas, T., 2017. Modular interior loading and exterior decoration of a virus-like particle. *Nanoscale* 9, 10420-10430. <https://doi.org/10.1039/C7NR03018E>.

Shin, M.D., Hochberg, J.D., Pokorski, J.K., Steinmetz, N.F., 2021. Bioconjugation of Active Ingredients to Plant Viral Nanoparticles Is Enhanced by Preincubation with a Pluronic F127 Polymer Scaffold. *ACS Appl Mater Interfaces* 13, 59618-59632. <https://doi.org/10.1021/acsami.1c13183>.

Shukla, S., Ablack, A.L., Wen, A.M., Lee, K.L., Lewis, J.D., Steinmetz, N.F., 2013. Increased Tumor Homing and Tissue Penetration of the Filamentous Plant Viral Nanoparticle Potato virus X. *Mol. Pharm.* 10, 33-42. <https://doi.org/10.1039/C7NR03018E>.

Shukla, S., Marks, I., Church, D., Chan, S.-K., Pokorski, J.K., Steinmetz, N.F., 2021. Tobacco mosaic virus for the targeted delivery of drugs to cells expressing prostate-specific membrane antigen. *RSC Adv.* 11, 20101-20108. <https://doi.org/10.1039/D1RA03166J>.

Shukla, S., Roe, A.J., Liu, R., Veliz, F.A., Commandeur, U., Wald, D.N., Steinmetz, N.F., 2020. Affinity of plant viral nanoparticle potato virus X (PVX) towards malignant B cells enables cancer drug delivery. *Biomater. Sci* 8, 3935-3943. <https://doi.org/10.1039/D0BM00683A>.

Shukla, S., Wen, A.M., Ayat, N.R., Commandeur, U., Gopalkrishnan, R., Broome, A.-M., Lozada, K.W., Keri, R.A., Steinmetz, N.F., 2014. Biodistribution and clearance of a filamentous plant virus in healthy and tumor-bearing mice. *Nanomedicine* 9, 221-235. <https://doi.org/10.1021/acs.biomac.8b01365>.

Sofi, H.S., Ashraf, R., Khan, A.H., Beigh, M.A., Majeed, S., Sheikh, F.A., 2019. Reconstructing nanofibers from natural polymers using surface functionalization approaches for applications in tissue engineering, drug delivery and biosensing devices. *Mater. Sci. Eng. C* 94, 1102-1124. <https://doi.org/10.1016/j.msec.2018.10.069>

Solomonov, A., Shimanovich, U., 2020. Self-Assembly in Protein-Based Bionanomaterials. *Isr. J. Chem.* 60, 1152-1170. <https://doi.org/10.1002/ijch.201900083>.

Steinmetz, N.F., 2010. Viral nanoparticles as platforms for next-generation therapeutics and imaging devices. *Nanomedicine NANOMED-NANOTECHNOL* 6, 634-641. <https://doi.org/10.1016/j.nano.2010.04.005>.

Steinmetz, N.F., Hong, V., Spoerke, E.D., Lu, P., Breitenkamp, K., Finn, M.G., Manchester, M., 2009. Buckyballs Meet Viral Nanoparticles: Candidates for Biomedicine. *J. Am. Chem. Soc.* 131, 17093-17095. <https://doi.org/10.1021/ja902293w>.

Steinmetz, N.F., Mertens, M.E., Taurog, R.E., Johnson, J.E., Commandeur, U., Fischer, R., Manchester, M., 2010. Potato virus X as a novel platform for potential biomedical applications. *Nano Lett* 10, 305-312. <https://doi.org/10.1021/nl9035753>.

Stephanopoulos, N., Carrico, Z.M., Francis, M.B., 2009. Nanoscale integration of sensitizing chromophores and porphyrins with bacteriophage MS2. *Angew Chem Int Ed Engl* 48, 9498-9502. <https://doi.org/10.1002/anie.200902727>.

Storni, T., Ruedl, C., Schwarz, K., Schwendener, R.A., Renner, W.A., Bachmann, M.F., 2004. Nonmethylated CG Motifs Packaged into Virus-Like Particles Induce Protective Cytotoxic T Cell Responses in the Absence of Systemic Side Effects. *J Immunol* 172, 1777. <https://doi.org/10.4049/jimmunol.172.3.1777>.

Stupka, I., Heddle, J.G., 2020. Artificial protein cages – inspiration, construction, and observation. *Curr. Opin. Struct.* 64, 66-73. <https://doi.org/10.1016/j.sbi.2020.05.014>.

Suci, P.A., Varpness, Z., Gillitzer, E., Douglas, T., Young, M., 2007. Targeting and Photodynamic Killing of a Microbial Pathogen Using Protein Cage Architectures Functionalized with a Photosensitizer. *Langmuir* 23, 12280-12286. <https://doi.org/10.1021/la7021424>.

Suffian, I.F.B.M., Al-Jamal, K.T., 2022. Bioengineering of virus-like particles as dynamic nanocarriers for in vivo delivery and targeting to solid tumours. *Adv Drug Deliv Revi.* 180, 114030. <https://doi.org/10.1016/j.addr.2021.114030>.

- Sun, H., Li, Y., Yu, S., Liu, J., 2020. Hierarchical Self-Assembly of Proteins Through Rationally Designed Supramolecular Interfaces. *Front. Bioeng. Biotechnol.* 8. <https://doi.org/10.3389/fbioe.2020.00295>.
- Sungsuwan, S., Wu, X., Huang, X., 2017. Chapter Thirteen - Evaluation of Virus-Like Particle-Based Tumor-Associated Carbohydrate Immunogen in a Mouse Tumor Model, in: Imperiali, B. (Ed.), *Methods in Enzymol.* Academic Press, pp. 359-376. <https://doi.org/10.1016/bs.mie.2017.06.030>.
- Tao, L., Kaddis, C.S., Loo, R.R., Grover, G.N., Loo, J.A., Maynard, H.D., 2009. Synthesis of Maleimide-End Functionalized Star Polymers and Multimeric Protein-Polymer Conjugates. *Macromolecules* 42, 8028-8033. <https://doi.org/10.1021/ma901540p>.
- Teng, M., Yao, Y., Nair, V., Luo, J., 2021. Latest Advances of Virology Research Using CRISPR/Cas9-Based Gene-Editing Technology and Its Application to Vaccine Development. *Viruses* 13. <https://doi.org/10.3390/v13050779>
- Thompson, C.M., Petiot, E., Lennaertz, A., Henry, O., Kamen, A.A., 2013. Analytical technologies for influenza virus-like particle candidate vaccines: challenges and emerging approaches. *Virol. J.* 10, 141. <https://doi.org/10.1186/1743-422X-10-141>.
- Tong, G.J., Hsiao, S.C., Carrico, Z.M., Francis, M.B., 2009. Viral capsid DNA aptamer conjugates as multivalent cell-targeting vehicles. *J Am Chem Soc.* 131, 11174-11178. <https://doi.org/10.1021/ja903857f>.
- Tuma, R., Prevelige, P.E., Jr., Thomas, G.J., Jr., 1996. Structural transitions in the scaffolding and coat proteins of P22 virus during assembly and disassembly. *Biochem* 35, 4619-4627. <https://doi.org/10.1021/bi952793l>.
- Tumban, E., Peabody, J., Tyler, M., Peabody, D.S., Chackerian, B., 2012. VLPs displaying a single L2 epitope induce broadly cross-neutralizing antibodies against human papillomavirus. *PloS one* 7, e49751. <https://doi.org/10.1371/journal.pone.0049751>.
- Twarock, R., Bingham, R.J., Dykeman, E.C., Stockley, P.G., 2018. A modelling paradigm for RNA virus assembly. *Curr Opin Virol* 31, 74-81. <https://doi.org/10.1016/j.coviro.2018.07.003>.
- Van Regenmortel, M.H.V., 2008. Tobacco Mosaic Virus, in: Mahy, B.W.J., Van Regenmortel, M.H.V. (Eds.), *Encyclopedia of Virology (Third Edition)*. Academic Press, Oxford, pp. 54-60.
- Vervoort, D.F.M., Heiringhoff, R., Timmermans, S.B.P.E., van Stevendaal, M.H.M.E., van Hest, J.C.M., 2021. Dual Site-Selective Presentation of Functional Handles on Protein-Engineered Cowpea Chlorotic Mottle Virus-Like Particles. *Bioconjugate Chem.* 32, 958-963. <https://doi.org/10.1021/acs.bioconjchem.1c00108>.
- Vilar, G., Tulla-Puche, J., Albericio, F., 2012. Polymers and drug delivery systems. *Curr Drug Deliv* 9, 367-394. <https://doi.org/10.2174/156720112801323053>
- Waghvani, H.K., Uchida, M., Fu, C.-Y., LaFrance, B., Sharma, J., McCoy, K., Douglas, T., 2020. Virus-Like Particles (VLPs) as a Platform for Hierarchical Compartmentalization. *Biomacromolecules* 21, 2060-2072. <https://doi.org/10.1021/acs.biomac.0c00030>.

- Wang, C., Beiss, V., Steinmetz, N.F., 2019. Cowpea Mosaic Virus Nanoparticles and Empty Virus-Like Particles Show Distinct but Overlapping Immunostimulatory Properties. *J Virol* 93. <https://doi.org/10.1128/JVI.00129-19>.
- Wang, C., Sun, W., Wright, G., Wang, A.Z., Gu, Z., 2016. Inflammation-Triggered Cancer Immunotherapy by Programmed Delivery of CpG and Anti-PD1 Antibody. *Adv Mater* 28, 8912-8920. <https://doi.org/10.1002/adma.201506312>.
- Wang, H., Dai, T., Zhou, S., Huang, X., Li, S., Sun, K., Zhou, G., Dou, H., 2017a. Self-Assembly Assisted Fabrication of Dextran-Based Nanohydrogels with Reduction-Cleavable Junctions for Applications as Efficient Drug Delivery Systems. *Sci. Rep.* 7, 40011. <https://doi.org/10.1038/srep40011>.
- Wang, H., Feng, Z., Xu, B., 2017b. Bioinspired assembly of small molecules in cell milieu. *Chem. Soc. Rev.* 46, 2421-2436. <https://doi.org/10.1039/C6CS00656F>.
- Wang, J., Hu, X., Xiang, D., 2018. Nanoparticle drug delivery systems: an excellent carrier for tumor peptide vaccines. *Drug Deliv.* 25, 1319-1327. <https://doi.org/10.1080%2F10717544.2018.1477857>.
- Wang, Q., Chan, T.R., Hilgraf, R., Fokin, V.V., Sharpless, K.B., Finn, M.G., 2003. Bioconjugation by Copper(I)-Catalyzed Azide-Alkyne [3 + 2] Cycloaddition. *J. Am. Chem. Soc.* 125, 3192-3193. <https://doi.org/10.1021/ja021381e>.
- Wang, Y., Wang, G., Duan, W.-T., Sun, M.-X., Wang, M.-H., Wang, S.-H., Cai, X.-H., Tu, Y.-b., 2020. Self-assembly into virus-like particles of the recombinant capsid protein of porcine circovirus type 3 and its application on antibodies detection. *AMB Express* 10, 3. <https://doi.org/10.1186%2Fs13568-019-0940-0>.
- Warzecha, H., Mason, H.S., Lane, C., Tryggvesson, A., Rybicki, E., Williamson, A.-L., Clements, J.D., Rose, R.C., 2003. Oral immunogenicity of human papillomavirus-like particles expressed in potato. *Journal of virology* 77, 8702-8711. <https://doi.org/10.1128%2FJVI.77.16.8702-8711.2003>.
- Wege, C., Geiger, F., 2018. Dual Functionalization of Rod-Shaped Viruses on Single Coat Protein Subunits, in: Wege, C., Lomonosoff, G.P. (Eds.), *Virus-Derived Nanoparticles for Advanced Technologies: Methods and Protocols*. Springer NY, pp. 405-424. [https://doi.org/10.1007/978-1-4939-7808-3\\_27](https://doi.org/10.1007/978-1-4939-7808-3_27).
- Weis, F., Beckers, M., von der Hocht, I., Sachse, C., 2019. Elucidation of the viral disassembly switch of tobacco mosaic virus. *EMBO reports* 20, e48451. <https://doi.org/10.15252/embr.201948451>.
- Welch, R.P., Lee, H., Luzuriaga, M.A., Brohlin, O.R., Gassensmith, J.J., 2018. Protein-Polymer Delivery: Chemistry from the Cold Chain to the Clinic. *Bioconjug. Chem.* 29, 2867-2883. <https://doi.org/10.1021/acs.bioconjchem.8b00483>.
- Wellink, J., 1998. Comovirus Isolation and RNA Extraction, in: Foster, G.D., Taylor, S.C. (Eds.), *Plant Virology Protocols: From Virus Isolation to Transgenic Resistance*. Humana Press, Totowa, NJ, pp. 205-209.

Wen, A.M., Lee, K.L., Cao, P., Pangilinan, K., Carpenter, B.L., Lam, P., Veliz, F.A., Ghiladi, R.A., Advincula, R.C., Steinmetz, N.F., 2016. Utilizing Viral Nanoparticle/Dendron Hybrid Conjugates in Photodynamic Therapy for Dual Delivery to Macrophages and Cancer Cells. *Bioconjug. Chem.* 27, 1227-1235. <https://doi.org/10.1021/acs.bioconjchem.6b00075>.

Wen, A.M., Shukla, S., Saxena, P., Aljabali, A.A.A., Yildiz, I., Dey, S., Mealy, J.E., Yang, A.C., Evans, D.J., Lomonosoff, G.P., Steinmetz, N.F., 2012. Interior Engineering of a Viral Nanoparticle and Its Tumor Homing Properties. *Biomacromolecules* 13, 3990-4001. <https://doi.org/10.1021/bm301278f>.

Wilts, B.D., Schaap, I.A.T., Schmidt, C.F., 2015. Swelling and softening of the cowpea chlorotic mottle virus in response to pH shifts. *Biophys J* 108, 2541-2549. <https://doi.org/10.1016%2Fj.bpj.2015.04.019>.

Wu, W., Hsiao, S.C., Carrico, Z.M., Francis, M.B., 2009. Genome-free viral capsids as multivalent carriers for taxol delivery. *Angew. Chem. Int. Ed. Engl.* 48, 9493-9497. <https://doi.org/10.1002/anie.200902426>.

Wu, Y., Yang, H., Jeon, Y.-J., Lee, M.-Y., Li, J., Shin, H.-J., 2014. Surface modification of cowpea chlorotic mottle virus capsids via a copper(I)-catalyzed azide-alkyne cycloaddition (CuAAC) reaction and their adhesion behavior with HeLa cells. *Biotechnol. Bioproc. E.* 19, 747-753. <https://doi.org/10.1007/s12257-014-0145-y>.

Wu, Z., Chen, K., Yildiz, I., Dirksen, A., Fischer, R., Dawson, P.E., Steinmetz, N.F., 2012. Development of viral nanoparticles for efficient intracellular delivery. *Nanoscale* 4, 3567-3576. <https://doi.org/10.1039/C2NR30366C>.

Xing, P., Zhao, Y., 2016. Multifunctional Nanoparticles Self-Assembled from Small Organic Building Blocks for Biomedicine. *Adv. Mater.* 28, 7304-7339. <https://doi.org/10.1002/adma.201600906>.

Yadav, S., Sharma, A.K., Kumar, P., 2020. Nanoscale Self-Assembly for Therapeutic Delivery. *Front. Bioeng. Biotechnol.* 8. <https://doi.org/10.3389%2Ffbioe.2020.00127>.

Yi, H., Nisar, S., Lee, S.-Y., Powers, M.A., Bentley, W.E., Payne, G.F., Ghodssi, R., Rubloff, G.W., Harris, M.T., Culver, J.N., 2005. Patterned Assembly of Genetically Modified Viral Nanotemplates via Nucleic Acid Hybridization. *Nano Lett.* 5, 1931-1936. <https://doi.org/10.1021/nl051254r>.

Yin, Z., Comellas-Aragones, M., Chowdhury, S., Bentley, P., Kaczanowska, K., Benmohamed, L., Gildersleeve, J.C., Finn, M.G., Huang, X., 2013. Boosting immunity to small tumor-associated carbohydrates with bacteriophage qbeta capsids. *ACS Chem. Biol.* 8, 1253-1262. <https://doi.org/10.1021%2Fcb400060x>.

Zdanowicz, M., Chroboczek, J., 2016. Virus-like particles as drug delivery vectors. *Acta Biochim. Pol.* 63, 469-473. [https://doi.org/10.18388/abp.2016\\_1275](https://doi.org/10.18388/abp.2016_1275).

Zeltins, A., 2013. Construction and characterization of virus-like particles: a review. *Mol. Biotechnol.* 53, 92-107. <https://doi.org/10.1007/s12033-012-9598-4>.

Zhao, L., Kopylov, M., Potter, C.S., Carragher, B., Finn, M.G., 2019. Engineering the PP7 Virus Capsid as a Peptide Display Platform. *ACS Nano* 13, 4443-4454. <https://doi.org/10.1021%2Facs.nano.8b09683>.

Zhao, X., Fox, J.M., Olson, N.H., Baker, T.S., Young, M.J., 1995. In Vitro Assembly of Cowpea Chlorotic Mottle Virus from Coat Protein Expressed in *Escherichia coli* and in Vitro-Transcribed Viral cDNA. *Virology* 207, 486-494. <https://doi.org/10.1006/viro.1995.1108>.

Zheng, Y., Lee, P.W., Wang, C., Thomas, L.D., Stewart, P.L., Steinmetz, N.F., Pokorski, J.K., 2019. Freeze-Drying To Produce Efficacious CPMV Virus-like Particles. *Nano Lett.* 19, 2099-2105. <https://doi.org/10.1021/acs.nanolett.9b00300>.

Zhou, K., Li, F., Dai, G., Meng, C., Wang, Q., 2013. Disulfide Bond: Dramatically Enhanced Assembly Capability and Structural Stability of Tobacco Mosaic Virus Nanorods. *Biomacromolecules* 14, 2593-2600. <https://doi.org/10.1021/bm400445m>.